

Time-dependent quantum transport through an interacting quantum dot beyond sequential tunneling: second-order quantum rate equations

Bing Dong, G. H. Ding, and X. L. Lei

*Key Laboratory of Artificial Structures and Quantum Control (Ministry of Education),
Department of Physics, Shanghai Jiaotong University, 800 Dongchuan Road, Shanghai 200240, China*
(Dated: November 24, 2014)

A general theoretical formulation for the effect of a strong on-site Coulomb interaction on the time-dependent electron transport through a quantum dot under the influence of arbitrary time-varying bias voltages and/or external fields is presented, based on slave bosons and the Keldysh nonequilibrium Green's function (GF) techniques. To avoid the difficulties of computing double-time GFs, we generalize the propagation scheme recently developed by Croy and Saalman to combine the auxiliary-mode expansion with the celebrated Lacroix's decoupling approximation in dealing with the second-order correlated GFs and then establish a closed set of coupled equations of motion, called second-order quantum rate equations (SOQREs), for exact description of transient dynamics of electron correlated tunneling. We verify that the stationary solution of our SOQREs is able to correctly describe the Kondo effect on a qualitative level. Moreover, a comparison with other methods, such as the second-order von Neumann approach and Hubbard-I approximation, is performed. As illustrations, we investigate the transient current behaviors in response to a step voltage pulse and a harmonic driving voltage, and linear admittance as well, in the cotunneling regime.

PACS numbers: 72.10.Bg, 73.23.Hk, 73.63.-b

I. INTRODUCTION

The dynamical response of conduction electrons in open nanostructures driven by time-dependent external fields has attracted tremendous interest in coherent quantum transport theory because of its potential application to quantum information processing and single-electron devices.^{1–13} In experiments, one is interested in measuring the current response of a mesoscopic system, usually a quantum dot (QD), driven by time-dependent periodic signals applied either on the system itself or on the attached leads, leading to the observation of the phenomena, such as quantum pumping^{5–8} and photon-assisted tunneling.^{9,14} An alternative way of external field modulation is to apply radio-frequency signals to the metallic gates that control the opening of the QD to its electrodes by oscillating tunneling barriers, i.e. a quantum dot turnstile.^{10–13} It is known that the fundamental physics of the nanoscale structures is dominated by two effects, the quantum coherence and electron correlations, which significantly affect the electronic tunneling through the nanostructures, giving rise to prototypical quantum phenomena, for instance, the Coulomb blockade and the Kondo effect. These time-resolved experiments have therefore motivated the theoretical investigations for transient current-response behavior of an interacting QD under influences of arbitrary time-varying external fields in the cotunneling and the Kondo regimes.

In literature, various theoretical methods have been developed to study these time-dependent nonequilibrium phenomena. The scattering matrix approaches can only be applicable for the noninteracting system.^{15,16} The nonequilibrium Green's function (NGF) methods are believed to be the most powerful method for investiga-

tion of nonequilibrium time-dependent transport problem in an arbitrary nanoscale device.^{17–32} For the case of noninteracting system, exact analytical solutions were obtained based on the time-dependent nonequilibrium Green's function (TDNGF) to the nonlinear transient current through a QD in response to sharp step- and square-shaped voltage pulses and harmonic bias modulations as well.^{17,20} For an interacting system, certain approximations have to be invoked to calculate the correlated GFs. For instance, the conventional perturbation theory in the on-site interaction strength U was developed to study the transient dynamics of the Anderson impurity model.^{28,32} A response of this model in the Kondo regime was examined by applying the time-dependent Schrieffer-Wolff transformation and combining with the perturbation theory,^{24–26} or using an interpolation of the retarded self-energy.²⁷ An exact analytical solution for a Kondo QD in response to a rectangular pulsed bias potential was also derived in the Toulouse point.³¹ Departure from this special point, numerical investigations on this issue were performed using time-dependent non-crossing approximation (NCA).^{29,30} In recent years, several advanced approaches that can deal with higher order dynamics have been developed based on the real-time quantum Monte Carlo and iterative path-integral methods,^{33–35} real-time density matrix renormalization group methods,^{36–38} etc. Albeit that these new methods are favorable in studying strong correlation effects, the validity of their application in the time-dependent nonequilibrium problem is still controversial.

The generalized quantum master equations (GQMEs) for the reduced density matrix,^{39–53} have the ability to cover the whole parameter regions of the interaction strength, from weak Coulomb interactions (sequential

tunneling in the Coulomb blockade regime),^{42–44,47,48} intermediate couplings (cotunneling),^{39,45,46,49,50,53} to strong Coulomb interactions (the Kondo-type tunneling),^{39,51} depending on which order in perturbation expansion with respect to the tunneling Hamiltonian is evaluated in the transport kernels. The real-time diagrammatic technique provides a systematic and unified scheme to handle any order of expansion terms in tunneling Hamiltonian and can be in principle exact for quantum transport.³⁹ This technique was then applied to study adiabatic and nonadiabatic pumping problems in a QD.^{40,41} It is nevertheless a formidable task to identify all diagrams involving higher order contributions in this formalism. Recently, an evaluation of the transport kernels up to fourth-order expansion was accomplished for the stationary tunneling, which can account for all processes involving coherent tunneling of one or two electrons.⁵³ Actually, certain kind of contributions beyond fourth-order transport kernels can be included by expanding equations of motion for the density matrix and the first-order auxiliary current matrices.⁴⁶ This second-order von Neumann (SOvN) approach however relies on the Markov limit, and then fails to describe the transient tunneling dynamics. A similar but more rigorous scheme was developed by the hierarchical equations of motion (HEOM) based on the influence functional in the path integral formalism.⁵⁰ For infinite levels the HEOM is exact and its second-tier approximation has been proven to be completely in agreement with the results by the real-time diagrammatic formalism at the same level.⁵⁰ Recently, the HEOM has been utilized to study the Kondo effect in the stationary tunneling.⁵¹ Therefore, a well developed and convenient theoretical formalism deserves to be further improved for the description of transient dynamics of strongly correlated nanoscale structures under arbitrary time-dependent external fields, and is currently a very active research area.

More recently, a general propagation scheme was developed by Croy and Saalmann for the transient problem in a noninteracting QD based on the TDNGF techniques.⁵⁴ In a similar fashion as the SOvN, they started from the equations of motion (EOMs) of the density matrix and auxiliary current matrices. By virtue of the TDNGF techniques and an auxiliary-mode expansion, the current matrices can then be expressed in a closed form. To this end, a set of coupled differential equations for quantities with only one time argument was obtained. In this way, this scheme avoids huge costs of numerical calculations in the traditional approaches, which compute directly the double-time GFs in time-domain requiring a double integration over time.^{19,22} Meanwhile, this scheme allows us to study arbitrary time dependences and structured reservoirs. This renders it an ideal tool for the time-dependent problem. Then this scheme was applied to study electron pumps⁵⁵ and time-dependent transport in molecular junctions.^{56–58} Moreover, this scheme was extended to the interacting case in the Hubbard-I

approximation.⁵⁹ The purpose of this paper is therefore to generalize this propagation scheme to account for the electron-electron interaction beyond this level of approximation, making it capable of investigating the strong correlation effects in time-dependent nonequilibrium situations, e.g. the cotunneling and dynamic Kondo-type tunneling.

The remainder of this paper is organized as follows. In Sec. II we introduce the time-dependent Anderson model Hamiltonian and its slave particle representation. In Sec. III we present the theoretical methodology. Starting from the EOM of density matrix, we define the auxiliary current matrices $\Pi_{\eta\sigma}(t)$ and then expand them in terms of auxiliary modes by employing a decomposition of the Fermi function and NGF technique in the wide band limit. Subsequently, we derive the EOM of the auxiliary-mode expansion of the current matrices, which will generate the next-order auxiliary density matrices (AMDEs) being related to the second-order correlated GFs due to the on-site Coulomb interaction. To truncate this procedure, a decoupling approximation has to be invoked. In this paper, we will utilize three decoupling approximations to calculate the second-order GFs, including the Hubbard-I approximation, the Lacroix's decoupling approximation,⁶⁰ and its simplified version.⁶¹ We find that the EOM of the current matrices is already closed at the Hubbard-I approximation and is consistent with the previous result.⁵⁹ While within the Lacroix's decoupling approximation, the whole procedure will be closed in the EOM of the second-order AMDEs. That is the reason that we call them as the second-order quantum rate equations (SOQREs). In Sec. IV, in order to appreciate our formalism, we use our resulting SOQREs to study the steady-state transport through an interacting QD in the Kondo regime and compare our results with the previous exact solutions of EOM of retarded GFs at the same level of approximation.^{62–64} In Sec. V, we apply our SOQREs to examine transient current in response to steplike and harmonic modulations of bias voltages, and ac linear response as well, in cotunneling regime. Finally, a conclusion is presented in Sec. VI.

II. MODEL HAMILTONIAN AND SLAVE-PARTICLE REPRESENTATION

We consider an interacting quantum dot with a single energy level connected to two normal metal leads, whose Hamiltonian can be separated as three parts:

$$H = H_C + H_{QD} + H_T. \quad (1)$$

The Hamiltonian H_C describes the noninteracting electrons in the two reservoirs, the left (L) and right (R) leads, and takes the following form:

$$H_C = \sum_{\eta k \sigma} \epsilon_{\eta k}(t) c_{\eta k \sigma}^\dagger c_{\eta k \sigma}, \quad (2)$$

where $\eta = \{L, R\}$ stands for lead index, k denotes electron momentum, and $\sigma = \{\uparrow, \downarrow\}$ is the spin orientation of electrons. Here $c_{\eta k \sigma}^\dagger$ and $c_{\eta k \sigma}$ are electron creation and annihilation operators for the electronic state $k\sigma$ in the lead η , respectively. Each of the two leads is separately in thermal equilibrium with the chemical potential μ_η , which is set to be zero in equilibrium condition and chosen as the energy reference throughout the paper. The QD Hamiltonian adopts the single-impurity Anderson model,

$$H_{QD} = \sum_{\sigma} \epsilon_{d\sigma}(t) c_{d\sigma}^\dagger c_{d\sigma} + U n_{d\uparrow} n_{d\downarrow}, \quad (3)$$

in which $c_{d\sigma}^\dagger$ and $c_{d\sigma}$ are creation and annihilation operators for a spin- σ electron with an energy $\epsilon_{d\sigma}(t)$ on the QD. $n_{d\sigma} = c_{d\sigma}^\dagger c_{d\sigma}$ is the occupation operator in the QD and U is the charge energy. In this paper, we assume that the charge energy is large enough to exclude the double occupancy of the dot level. The last term H_T describes the tunnel coupling between the QD and two electrodes,

$$H_T = \sum_{\eta k \sigma} \left(V_{\eta k \sigma}(t) c_{\eta k \sigma}^\dagger c_{d\sigma} + \text{H.c.} \right), \quad (4)$$

with the coupling matrix element $V_{\eta k \sigma}(t)$. Here to model time-dependent transport problem subject to arbitrary time-varying bias and/or gate voltages, the single-particle energies in the dot $\epsilon_{d\sigma}(t)$, in the leads $\epsilon_{\eta k}(t)$, and the coupling matrix element $V_{\eta k \sigma}(t)$ are introduced to be all time dependent and independent of each other: $\epsilon_{d\sigma}(t) = \epsilon_{0\sigma} + \Delta_d(t)$, $\epsilon_{\eta k}(t) = \epsilon_{\eta k}^0 + \Delta_\eta(t)$, and $V_{\eta k \sigma}(t) = u_\eta(t) V_{\eta k \sigma}^0$. Without loss of generality, we assume that $\Delta_d(t)$, $\Delta_\eta(t)$, and $u_\eta(t)$ are all real functions of time. Throughout we will use natural units $e = \hbar = k_B = 1$.

According to the infinite- U slave-boson representation,⁶⁵ the electron operator $c_{d\sigma}$ can be written in three possible single electron states, namely: the empty state $|0\rangle$ with zero energy $\epsilon_0 = 0$, the singly occupied (with spin up or down) electronic state $|\sigma\rangle$, as

$$c_{d\sigma} = |0\rangle\langle\sigma|. \quad (5)$$

Because these three states expand the entire Hilbert space, the completeness relation must be satisfied

$$|0\rangle\langle 0| + \sum_{\sigma} |\sigma\rangle\langle\sigma| = 1. \quad (6)$$

These Dirac brackets were then treated as operators: $b^\dagger = |0\rangle$ as slave-boson operator and $f_\sigma^\dagger = |\sigma\rangle$ as pseudo-fermion operator. In terms of these auxiliary operators, Eqs.(5) and (6) become

$$c_{d\sigma} = b^\dagger f_\sigma, \quad (7)$$

$$b^\dagger b + \sum_{\sigma} f_\sigma^\dagger f_\sigma = 1. \quad (8)$$

The explicit (anti)commutators of these auxiliary particles can be easily established from the definitions of the

Dirac brackets:⁶⁶

$$bb^\dagger = 1, f_\sigma f_{\sigma'}^\dagger = \delta_{\sigma\sigma'}, b f_\sigma^\dagger = f_\sigma b^\dagger = 0. \quad (9)$$

Therefore, using these new fermionic and slave-bosonic operators, the QD and tunneling Hamiltonians (3) and (4) can be rewritten, respectively, as:

$$H_{QD} = \sum_{\sigma} \epsilon_{d\sigma}(t) f_\sigma^\dagger f_\sigma, \\ H_T = \sum_{\eta k \sigma} [V_{\eta k \sigma}(t) c_{\eta k \sigma}^\dagger b^\dagger f_\sigma + \text{H.c.}]. \quad (10)$$

Furthermore, as far as the three possible single electric states are considered as the basis, the expectation values of the diagonal elements of the density matrix, $\rho_{\alpha\alpha}$ ($\alpha = \{0, \sigma\}$), give the occupation probabilities of the resonant level in the QD being empty, or singly occupied by spin- σ electron, respectively. In the slave particle notation, the corresponding relations between the density matrix elements and these auxiliary operators are obvious as $\hat{\rho}_{00} = |0\rangle\langle 0| = b^\dagger b$, $\hat{\rho}_{\sigma\sigma} = |\sigma\rangle\langle\sigma| = f_\sigma^\dagger f_\sigma$. According to Eq. (8), we have

$$\rho_{00} + \sum_{\sigma} \rho_{\sigma\sigma} = 1. \quad (11)$$

III. THEORETICAL METHODS

In this section, we derive the second-order quantum rate equations (SOQREs) to describe the higher-order tunneling processes of an interacting QD modeled by Eq. (1) subject to arbitrary time-dependent potentials. Since one of the most important observables in the transport problem are the electron occupation number $\rho_{\alpha\alpha}(t)$ in the central region, we start from the Heisenberg EOM of the density matrix element:

$$i\dot{\rho}_{\sigma\sigma}(t) = \langle [f_\sigma^\dagger f_\sigma(t), H(t)] \rangle \\ = \sum_{\eta k} V_{\eta k \sigma}(t) \left[\langle f_\sigma^\dagger b(t) c_{\eta k \sigma}(t) - c_{\eta k \sigma}^\dagger(t) b^\dagger f_\sigma(t) \rangle \right]. \quad (12)$$

Another important observable is the current $I_\eta(t)$ from one of the electrodes to the central region under nonequilibrium condition, which is defined as the time evolution of the occupation number operator of the given lead:

$$I_\eta(t) = -e \langle \dot{N}_\eta \rangle = -\frac{ie}{\hbar} \langle [H, N_\eta] \rangle,$$

with $N_\eta = \sum_{k\sigma} c_{\eta k \sigma}^\dagger c_{\eta k \sigma}$. Since H_C and H_{QD} commute with N_η , one readily finds

$$I_\eta(t) = \frac{ie}{\hbar} \sum_{k\sigma} V_{\eta k \sigma}(t) \left[\langle c_{\eta k \sigma}^\dagger(t) b^\dagger f_\sigma(t) - f_\sigma^\dagger b(t) c_{\eta k \sigma}(t) \rangle \right]. \quad (13)$$

By defining the first-order ADMEs, the current matrices, $\hat{\Pi}_{\eta\sigma}(t)$, as

$$\hat{\Pi}_{\eta\sigma}(t) = i \sum_k V_{\eta k\sigma}(t) c_{\eta k\sigma}^\dagger(t) b^\dagger f_\sigma(t), \quad (14)$$

we can write the EOM of density matrix element Eq. (12) and the current Eq. (13) in term of the expectation value of the current matrices, $\Pi_{\eta\sigma}(t) = \langle \hat{\Pi}_{\eta\sigma}(t) \rangle$, as

$$\dot{\rho}_{\sigma\sigma}(t) = \sum_\eta [\Pi_{\eta\sigma}(t) + \Pi_{\eta\sigma}^\dagger(t)], \quad (15)$$

$$I_\eta(t) = \frac{e}{\hbar} \sum_\sigma [\Pi_{\eta\sigma}(t) + \Pi_{\eta\sigma}^\dagger(t)]. \quad (16)$$

Therefor, one has to calculate the current matrices by solving its own EOM, which will unavoidably cause some new unknown observables, second-order ADMEs, due to the existence of Coulomb interaction in the central region. This procedure will generate an infinite hierarchy of coupled EOMs for these ADMEs. In order to form a closed set of equations, some suitable decoupling approximations have to be invoked to break this hierarchy at certain level. The choice of an appropriate truncation procedure is critical in order to treat properly the strong correlation effects both from the on-site Coulomb interaction and from the dot-lead tunnel couplings. Several years ago, a SOvN approach was derived for electronic coherent transport through an interacting QD by only considering two-electron coherent tunneling processes and taking the Markov limit for the two-electron transition events.⁴⁶ This SOvN approach is believed to be in full agreement with the method of the diagrammatic real-time perturbation theory and to be able to describe correlated two-electron tunneling, cotunneling, because the current is calculated to higher order in the lead-dot coupling in this approach. However, the SOvN approach only works for temperatures above the Kondo temperature and gives incorrect time evolution behaviors of the tunneling current and electron occupancies. In this paper, we want to overcome the two drawbacks. First, a systematic and physically more clear decoupling approximation is introduced, e.g. the famous Lacroix's decoupling approximation,⁶⁰ to tackle the electronic correlation. Especially different from the SOvN approach, the present SOQREs will contain the back-action effect of the kinetics of the QD to the electrodes. Second, our approach allows for easy incorporation for arbitrary time-dependent effects in higher order quantum transport through an interacting QD. For these purposes, we will, in the following, generalize the recently developed TDNGF method with auxiliary-mode expansion to the interacting case.

A. Current matrices and its auxiliary-mode expansion

The key quantity is here the current matrices defined in Eq. (14). By applying the TDNGF with the Langreth's

analytic continuation rules, its expectation value can be expressed in terms of the Keldysh GFs of the QD as

$$\begin{aligned} \Pi_{\eta\sigma}(t) &= \sum_k V_{\eta k\sigma}(t) G_{\sigma, \eta k\sigma}^<(t, t) \\ &= \sum_k V_{\eta k\sigma}(t) \int_{-\infty}^t dt_1 V_{\eta k\sigma}^*(t_1) [G_\sigma^r(t, t_1) \\ &\quad \times g_{\eta k\sigma}^<(t_1, t) + G_\sigma^<(t, t_1) g_{\eta k\sigma}^a(t_1, t)] \\ &= \int_{-\infty}^t dt_1 [G_\sigma^>(t, t_1) \Sigma_{\eta\sigma}^<(t_1, t) \\ &\quad - G_\sigma^<(t, t_1) \Sigma_{\eta\sigma}^>(t_1, t)]. \end{aligned} \quad (17)$$

The superscripts $<, >$ denote the lesser or greater indices and r, a denote the retarded or advanced indices of these two-time functions. $G_{\sigma, \eta k\sigma}(t, t')$ and $G_\sigma(t, t')$ are the mixture GF and the GFs of the QD, respectively, which are defined using Zubarev's notation as: $G_{\sigma, \eta k\sigma}^\nu(t, t') = \langle \langle b^\dagger f_\sigma(t) | c_{\eta k\sigma}^\dagger(t') \rangle \rangle^\nu$, and $G_\sigma^\nu(t, t') = \langle \langle b^\dagger f_\sigma(t) | f_\sigma^\dagger b(t') \rangle \rangle^\nu$ ($\nu = \{<, >, r, a\}$). $g_{\eta k\sigma}(t, t')$ are the exact time-dependent GFs in the leads for the uncoupled system:

$$\begin{aligned} g_{\eta k\sigma}^<(t, t') &\equiv i \langle c_{\eta k\sigma}^\dagger(t') c_{\eta k\sigma}(t) \rangle \\ &= i f_\eta(\epsilon_{\eta k}^0) \exp \left[-i \int_{t'}^t d\tau \epsilon_{\eta k}(\tau) \right], \end{aligned} \quad (18)$$

$$\begin{aligned} g_{\eta k\sigma}^>(t, t') &\equiv -i \langle c_{\eta k\sigma}(t) c_{\eta k\sigma}^\dagger(t') \rangle \\ &= -i [1 - f_\eta(\epsilon_{\eta k}^0)] \exp \left[-i \int_{t'}^t d\tau \epsilon_{\eta k}(\tau) \right], \end{aligned} \quad (19)$$

$$\begin{aligned} g_{\eta k\sigma}^{r,a}(t, t') &\equiv \mp i \theta(\pm t \mp t') \langle \{ c_{\eta k\sigma}(t), c_{\eta k\sigma}^\dagger(t') \} \rangle \\ &= \mp i \theta(\pm t \mp t') \exp \left[-i \int_{t'}^t d\tau \epsilon_{\eta k}(\tau) \right], \end{aligned} \quad (20)$$

where $f_\eta(\epsilon)$ is the Fermi distribution function of the lead η with the chemical potential μ_η and the temperature T [$\beta = (k_B T)^{-1}$],

$$f_\eta(\epsilon) = \frac{1}{1 + e^{\beta(\epsilon - \mu_\eta)}}.$$

$\Sigma_{\eta\sigma}^{<(>)}(t_1, t)$ are the corresponding self-energies of the QD due to tunnel-coupling to electrode η :

$$\begin{aligned} \Sigma_{\eta\sigma}^<(t_1, t) &= \sum_k V_{\eta k\sigma}^*(t_1) g_{\eta k\sigma}^<(t_1, t) V_{\eta k\sigma}(t) \\ &= i \int \frac{d\epsilon}{2\pi} f_\eta(\epsilon) e^{-i\epsilon(t_1 - t)} \Gamma_{\eta\sigma}(\epsilon, t_1, t), \end{aligned} \quad (21)$$

$$\begin{aligned} \Sigma_{\eta\sigma}^>(t_1, t) &= \sum_k V_{\eta k\sigma}^*(t_1) g_{\eta k\sigma}^>(t_1, t) V_{\eta k\sigma}(t) \\ &= -i \int \frac{d\epsilon}{2\pi} f_\eta^-(\epsilon) e^{-i\epsilon(t_1 - t)} \Gamma_{\eta\sigma}(\epsilon, t_1, t) \end{aligned} \quad (22)$$

with $f_\eta^-(\epsilon) = 1 - f_\eta(\epsilon)$. The generalized level-width function $\Gamma_{\eta\sigma}(\epsilon, t, t')$ depends on the density of states $\varrho_\eta(\epsilon)$ of lead η and the coupling $V_{\eta\sigma}(\epsilon, t) = V_{\eta k\sigma}(t)$

$$\Gamma_{\eta\sigma}(\epsilon, t_1, t) = 2\pi \varrho_\eta(\epsilon) V_{\eta\sigma}(\epsilon, t) V_{\eta\sigma}^*(\epsilon, t_1)$$

$$\times \exp \left[i \int_{t_1}^t d\tau \Delta_\eta(\tau) \right]. \quad (23)$$

To obtain the third equality in Eq. (17), we employ the relation for the two-time functions, the Green's functions and the self-energies, defined on the time forward and backward branches:

$$X^{r,a}(t, t') = \pm \theta(\pm t \mp t') [X^>(t, t') - X^<(t, t')]. \quad (24)$$

For further calculation of the self-energies, the detail information about the linewidth function containing the density of states $\rho_\eta(\varepsilon)$ and the energy-dependent tunneling matrix element $V_{\eta\sigma}(\varepsilon)$ have to be given as a input from the realistic first-principles calculation or be set as a specific toy model. Actually, two theoretical models are usually used in the context of quantum transport problem. One is the Lorentzian-form linewidth function,

$$\Gamma_{\eta\sigma}(\varepsilon) = 2\pi \rho_\eta(\varepsilon) V_{\eta\sigma}(\varepsilon) V_{\eta\sigma}^*(\varepsilon) = \frac{\Gamma_{\eta\sigma}^0 W^2}{\varepsilon^2 + W^2}, \quad (25)$$

with the linewidth amplitude $\Gamma_{\eta\sigma}^0$ and the bandwidth W . Lorentzian linewidth is believed to provide a mathematically convenient way to introduce finite-bandwidth effects on electronic transport through nanoscale device. The other simpler one is the so-called wideband limit (WBL), which is valid when the density of states in the leads varies slowly with energy in the vicinity of the levels of the central region. In this limit, the density of states of the lead η , ρ_η , and the coupling between the leads and the central region, $V_{\eta\sigma}^0$, are both assumed to be constant in the energy window relevant for transport. Obviously, this results in a tremendous simplification of mathematical calculation. Here, in order to concentrate our attention on the main objective of this paper, the correlation effect on higher order electronic tunneling through a QD, we chose the WBL in the following calculation. Therefore, the generalized linewidth function Eq. (23) becomes energy independence, $\Gamma_{\eta\sigma}(\varepsilon, t_1, t) = \Gamma_{\eta\sigma}(t_1, t)$ and

$$\Gamma_{\eta\sigma}(t_1, t) = \Gamma_{\eta\sigma}^0 u_\eta(t) u_\eta^*(t_1) \exp \left[i \int_{t_1}^t d\tau \Delta_\eta(\tau) \right], \quad (26)$$

with a constant tunnel-coupling strength $\Gamma_{\eta\sigma}^0 = 2\pi \sum_k |V_{\eta k\sigma}^0|^2 \delta(\varepsilon - \epsilon_{\eta k}^0)$. Nevertheless, it should be noted that our methodology is also applicable if the Lorentzian linewidth function is utilized.

Moreover, the next key skill is to derive analytical expressions for the self-energies Eqs. (21) and (22), i.e., the integral kernel of the current matrices in Eq. (17), by evaluating integrals involving the Fermi distribution function. Such expressions will needless to say significantly cut down the heavy computational burden for the simulations of transient response. In literature, the Matsubara expansion of the Fermi function has usually been applied for energy integrals by means of contour integration using the residue theorem. However, its slow

convergence makes it not suitable for numerical applications in fermionic many-body theory and time evolution problems in the present investigation. Recently, several highly accurate and much more efficient approximations have been proposed for the Fermi function, such as the continued fraction representation,⁶⁷ the partial fractional decomposition,^{56,68} and the Padé spectral decomposition.^{57,69,70} All of these decompositions have similar mathematical structure with the usual Matsubara expansion, that is an infinite summation over simple poles which are all located on the imaginary axis. As a result, these decompositions can be easily incorporated into many applications with the same procedure as for the Matsubara summation. In particular, the partial fractional decomposition was recently used by Croy and Saalman to transform the integration formula of the current matrices, Eq. (17), into the summation form, the auxiliary-mode expansion as is called by them, in the context of time dependent electron transport in a noninteracting QD. Here we will use one more efficient approximation, the Padé approximation, to expand the Fermi function as follows:^{69,70}

$$f_\eta(\varepsilon) \simeq \frac{1}{2} - \sum_{p=1}^{N_p} \frac{R_p}{\beta} \left(\frac{1}{\varepsilon - \chi_{\eta p}^+} + \frac{1}{\varepsilon - \chi_{\eta p}^-} \right), \quad (27)$$

where R_p is the p th residue in the Padé decomposition, and $\chi_{\eta p}^\pm = \mu_\eta \pm i\chi_p/\beta$, $i\chi_p$ is the p th Padé pole in the upper complex plane, i.e., $\chi_p > 0$ (see the Appendix for the detail of how to calculate these parameters). N_p is the number of Padé pole pairs.

Substituting the energy-independent linewidth function, Eq. (26), and the Padé expansion of the Fermi distribution function, Eq. (27), into the lesser and greater self-energies, Eqs. (21) and (22), the energy integration can be accomplished by applying contour integration and the Cauchy's residue theorem, and these self-energies can thus be transformed into the summation forms

$$\Sigma_{\eta\sigma}^{\lessgtr}(t_1, t) = \pm i \frac{1}{2} \Gamma_{\eta\sigma}^0 |u_\eta(t)|^2 \delta(t_1 - t) + u_\eta(t) \sum_p \Sigma_{\eta\sigma p}^+(t_1, t), \quad (28)$$

with

$$\Sigma_{\eta\sigma p}^+(t_1, t) = u_\eta^*(t_1) \frac{R_p}{\beta} \Gamma_{\eta\sigma}^0 e^{i \int_{t_1}^t d\tau \chi_{\eta p}^+(\tau)}, \quad (29)$$

for $t_1 < t$, and

$$\Sigma_{\eta\sigma}^{\lessgtr}(t_1, t) = \pm i \frac{1}{2} \Gamma_{\eta\sigma}^0 |u_\eta(t)|^2 \delta(t_1 - t) - u_\eta^*(t_1) \sum_p \Sigma_{\eta\sigma p}^-(t_1, t), \quad (30)$$

with

$$\Sigma_{\eta\sigma p}^-(t_1, t) = u_\eta(t) \frac{R_p}{\beta} \Gamma_{\eta\sigma}^0 e^{i \int_{t_1}^t d\tau \chi_{\eta p}^-(\tau)}, \quad (31)$$

for $t_1 > t$, respectively. Here $\chi_{\eta p}^\pm(t) = \chi_{\eta p}^\pm + \Delta_\eta(t)$. Then,

we insert the expanded self-energies into Eq. (17) to get

$$\Pi_{\eta\sigma}(t) = \frac{1}{4}\Gamma_{\eta\sigma}^0|u_{\eta}(t)|^2(\rho_{00} - \rho_{\sigma\sigma}) + u_{\eta}(t) \sum_p \Pi_{\eta\sigma p}(t), \quad (32)$$

and an *auxiliary-mode expansion* of the current matrices, $\Pi_{\eta\sigma p}(t)$,

$$\begin{aligned} \Pi_{\eta\sigma p}(t) &= \int_{-\infty}^t dt_1 \Sigma_{\eta\sigma p}^+(t_1, t) [G_{\sigma}^>(t, t_1) - G_{\sigma}^<(t, t_1)] \\ &= \int_{-\infty}^t dt_1 \Sigma_{\eta\sigma p}^+(t_1, t) [G_{\sigma}^r(t, t_1) - G_{\sigma}^a(t, t_1)]. \end{aligned} \quad (33)$$

To obtain Eq. (32), we use $G_{\sigma}^<(t, t) = i\rho_{\sigma\sigma}$ and $G_{\sigma}^>(t, t) = -i\rho_{00}$ according to the definition of the contour-ordered GFs. Likewise, it is easy to find

$$\Pi_{\eta\sigma}^{\dagger}(t) = \frac{1}{4}\Gamma_{\eta\sigma}^0|u_{\eta}(t)|^2(\rho_{00} - \rho_{\sigma\sigma}) + u_{\eta}^*(t) \sum_p \Pi_{\eta\sigma p}^*(t), \quad (34)$$

and

$$\Pi_{\eta\sigma p}^*(t) = \int_{-\infty}^t dt_1 \Sigma_{\eta\sigma p}^-(t, t_1) [G_{\sigma}^<(t_1, t) - G_{\sigma}^>(t_1, t)], \quad (35)$$

because of $[G_{\sigma}^{\pm}(t, t')]^{\dagger} = -G_{\sigma}^{\pm}(t', t)$ and $(\chi_{\eta p}^-)^* = \chi_{\eta p}^+$.

B. Equations of motion for $\Pi_{\eta\sigma p}$ and the second-order ADME

Performing time derivative of Eq. (33) yields

$$\begin{aligned} i\frac{\partial}{\partial t}\Pi_{\eta\sigma p}(t) &= u_{\eta}^*(t)\frac{R_p}{\beta}\Gamma_{\eta\sigma}^0(\rho_{00} + \rho_{\sigma\sigma}) - \chi_{\eta p}^+(t)\Pi_{\eta\sigma p}(t) \\ &+ \int_{-\infty}^t dt_1 \Sigma_{\eta\sigma p}^+(t_1, t) i\frac{\partial}{\partial t} [G_{\sigma}^r(t, t_1) - G_{\sigma}^a(t, t_1)] \end{aligned} \quad (36)$$

This equation shows that the EOM for the auxiliary-mode expansion of the current matrices relies on the EOMs for the retarded and advance GFs of the QD,

$$\begin{aligned} i\frac{\partial}{\partial t}G_{\sigma}^{r(a)}(t, t_1) &= \delta(t - t_1)\langle\{b^{\dagger}f_{\sigma}(t), f_{\sigma}^{\dagger}b(t)\}\rangle \\ &+ \langle\langle[b^{\dagger}f_{\sigma}(t), H(t)]|f_{\sigma}^{\dagger}b(t_1)\rangle\rangle^{r(a)} \\ &= [\rho_{00}(t) + \rho_{\sigma\sigma}(t)]\delta(t - t_1) + \epsilon_{d\sigma}(t)G_{\sigma}^{r(a)}(t, t_1) \\ &+ \sum_{\eta'k'} \left\{ V_{\eta'k'\sigma}^*(t) \left[G_{\eta'k'\sigma,\sigma}^{r(a)}(t, t_1) - G_{\eta'k'\sigma,\sigma}^{\bar{\sigma}\bar{\sigma},r(a)}(t, t_1) \right] \right. \\ &\quad \left. + V_{\eta'k'\bar{\sigma}}^*(t)G_{\eta'k'\bar{\sigma},\sigma}^{\bar{\sigma}\bar{\sigma},r(a)}(t, t_1) \right\}, \end{aligned} \quad (37)$$

where three new GFs appear in the last equality: the mixture GF $G_{\eta'k'\sigma,\sigma}^{\nu}(t, t') = \langle\langle c_{\eta'k'\sigma}(t)|f_{\sigma}^{\dagger}b(t')\rangle\rangle^{\nu}$ due to coupling to electrodes, and the two two-particle mixture GF $G_{\eta'k'\sigma_1,\sigma}^{\sigma_2\sigma_3,\nu}(t, t') = \langle\langle f_{\sigma_2}^{\dagger}(t)f_{\sigma_3}(t)c_{\eta'k'\sigma_1}(t)|f_{\sigma}^{\dagger}b(t')\rangle\rangle^{\nu}$ generated by the on-site Coulomb interaction inside the QD.

Following standard EOM analysis, one can easily derive the Dyson equation for the mixture GF,

$$G_{\eta'k'\sigma,\sigma}^{r(a)}(t, t_1) = \int dt_2 g_{\eta'k'\sigma}^{r(a)}(t, t_2) V_{\eta'k'\sigma}(t_2) G_{\sigma}^{r(a)}(t_2, t_1). \quad (38)$$

Substituting Eq. (37) into the equation Eq. (36) and applying Eq. (38), we get

$$\begin{aligned} i\frac{\partial}{\partial t}\Pi_{\eta\sigma p}(t) &= u_{\eta}^*(t)\frac{R_p}{\beta}\Gamma_{\eta\sigma}^0(\rho_{00} + \rho_{\sigma\sigma}) \\ &+ \left[\epsilon_{d\sigma}(t) - \frac{i}{2}\Gamma_{\sigma}(t) - \chi_{\eta p}^+(t) \right] \Pi_{\eta\sigma p}(t) \\ &+ \sum_{\eta'} [\Omega_{\eta\sigma p, \eta'1}(t) - \Omega_{\eta\sigma p, \eta'2}(t)], \end{aligned} \quad (39)$$

where $\Gamma_{\sigma}(t) = \sum_{\eta'} |u_{\eta'}(t)|^2 \Gamma_{\eta'\sigma}^0$, and two new second-order ADMEs $\Omega_{\eta\sigma p, \eta'\alpha}(t)$ ($\alpha = 1, 2$) are introduced as

$$\begin{aligned} \Omega_{\eta\sigma p, \eta'1}(t) &= \int_{-\infty}^t dt_1 \Sigma_{\eta\sigma p}^+(t_1, t) \sum_{k'} V_{\eta'k'\bar{\sigma}}^*(t) \\ &\times \left[G_{\eta'k'\bar{\sigma},\sigma}^{\bar{\sigma}\bar{\sigma},r}(t, t_1) - G_{\eta'k'\bar{\sigma},\sigma}^{\bar{\sigma}\bar{\sigma},a}(t, t_1) \right], \end{aligned} \quad (40)$$

$$\begin{aligned} \Omega_{\eta\sigma p, \eta'2}(t) &= \int_{-\infty}^t dt_1 \Sigma_{\eta\sigma p}^+(t_1, t) \sum_{k'} V_{\eta'k'\sigma}^*(t) \\ &\times \left[G_{\eta'k'\sigma,\sigma}^{\bar{\sigma}\bar{\sigma},r}(t, t_1) - G_{\eta'k'\sigma,\sigma}^{\bar{\sigma}\bar{\sigma},a}(t, t_1) \right]. \end{aligned} \quad (41)$$

For the case of noninteracting system, the second-order ADMEs are vanishing in the WBL, and thus the equations (15), (32), (34), and (39) together with the normalization relation Eq. (11) already constitute the closed set of coupled EOMs, which are exactly the same as those derived by Croy and Saalman.⁵⁴ While for an interacting QD under present study, one needs to make some approximations to calculate the second order GFs.

1. Hubbard-I approximation

First, we employ the Hartree-Fock approximation for the second order GF:

$$\begin{aligned} G_{\eta'k'\sigma_1,\sigma}^{\sigma_2\sigma_3,\nu}(t, t_1) &= \langle\langle f_{\sigma_2}^{\dagger}(t)f_{\sigma_3}(t)c_{\eta'k'\sigma_1}(t)|f_{\sigma}^{\dagger}b(t')\rangle\rangle^{\nu} \\ &\approx \langle\langle f_{\sigma_2}^{\dagger}(t)f_{\sigma_3}(t)\rangle\rangle\langle\langle c_{\eta'k'\sigma_1}(t)|f_{\sigma}^{\dagger}b(t')\rangle\rangle^{\nu} \\ &= \delta_{\sigma_2\sigma_3}\rho_{\sigma_2\sigma_2}(t)\delta_{\sigma_1\sigma}G_{\eta'k'\sigma,\sigma}^{\nu}(t, t_1). \end{aligned}$$

In this case, we can readily obtain the retarded GF of the QD, from Eq. (37), in the frequency domain,

$$G_{\sigma}^r(\varepsilon) = \frac{1 - \rho_{\bar{\sigma}\bar{\sigma}}}{\varepsilon - \epsilon_{0\sigma} + \frac{i}{2}\Gamma_{\sigma}(1 - \rho_{\bar{\sigma}\bar{\sigma}})}, \quad (42)$$

for the time-independent situation. This is usually referred to as the Hubbard-I approximation (HIA) in the context of the GF theory for strongly correlated electron systems. Thus, the EOM for the current matrices is also closed and takes the form

$$i\frac{\partial}{\partial t}\Pi_{\eta\sigma p}(t) = u_{\eta}^*(t)\frac{R_p}{\beta}\Gamma_{\eta\sigma}^0(1 - \rho_{\bar{\sigma}\bar{\sigma}})$$

$$+ \left[\epsilon_{d\sigma}(t) - \frac{i}{2} \Gamma'_\sigma(t) - \chi_{\eta p}^+(t) \right] \Pi_{\eta\sigma p}(t), \quad (43)$$

with $\Gamma'_\sigma(t) = \sum_{\eta'} |u_{\eta'}(t)|^2 (1 - \rho_{\bar{\sigma}\bar{\sigma}}(t)) \Gamma_{\eta'\sigma}^0$. Worth noticing that the resulting EOM Eq. (43) is similar with that derived by using EOM for operators, except for the extra factor $1 - \rho_{\bar{\sigma}\bar{\sigma}}(t)$ in $\Gamma'_\sigma(t)$ in our result. Removing the factor $1 - \rho_{\bar{\sigma}\bar{\sigma}}$ and spin indices in Eq. (43), this equation reduces exactly to the previously developed EOM for the current matrices of the noninteracting single-level QD system in the WBL.⁵⁴

It is known that the HIA is reasonable at relatively high temperatures, where the Kondo resonance does not appear during electron tunneling processes, at $T \gg T_K$ (T_K is the Kondo temperature). However, to investigate the system at low temperatures, where the higher order coherent tunneling (cotunneling) is the dominating transport mechanism involving two-electron correlated scattering processes, and even the Kondo effect plays a certain role, it is necessary to calculate the second order GF beyond this level of approximation.

2. Lacroix's decoupling approximation

At first, we derive the EOMs of the second order GFs, which will generate three third order GFs,

$$i \frac{\partial}{\partial t} G_{\eta'k'\bar{\sigma},\sigma}^{\bar{\sigma}\sigma,r}(t, t_1) = -\langle f_{\bar{\sigma}}^\dagger b c_{\eta'k'\bar{\sigma}}(t) \rangle \delta(t - t_1) + [\epsilon_{\eta'k'}(t) + \epsilon_{d\sigma}(t) - \epsilon_{d\bar{\sigma}}(t)] G_{\eta'k'\bar{\sigma},\sigma}^{\bar{\sigma}\sigma,r}(t, t_1)$$

$$+ \sum_{\eta''k''} V_{\eta''k''\bar{\sigma}}(t) \langle \langle c_{\eta''k''\bar{\sigma}}^\dagger(t) c_{\eta'k'\bar{\sigma}}(t) b^\dagger f_\sigma(t) | f_\sigma^\dagger b(t_1) \rangle \rangle^r - \sum_{\eta''k''} V_{\eta''k''\sigma}^*(t) \langle \langle f_{\bar{\sigma}}^\dagger b(t) c_{\eta'k'\bar{\sigma}}(t) c_{\eta''k''\sigma}(t) | f_\sigma^\dagger b(t_1) \rangle \rangle^r,$$

$$i \frac{\partial}{\partial t} G_{\eta'k'\sigma,\sigma}^{\bar{\sigma}\bar{\sigma},r}(t, t_1) = \epsilon_{\eta'k'}(t) G_{\eta'k'\sigma,\sigma}^{\bar{\sigma}\bar{\sigma},r}(t, t_1) + \sum_{\eta''k''} V_{\eta''k''\bar{\sigma}}(t) \langle \langle c_{\eta''k''\bar{\sigma}}^\dagger(t) c_{\eta'k'\sigma}(t) b^\dagger f_{\bar{\sigma}}(t) | f_\sigma^\dagger b(t_1) \rangle \rangle^r + \sum_{\eta''k''} V_{\eta''k''\sigma}^*(t) \langle \langle f_{\bar{\sigma}}^\dagger b(t) c_{\eta''k''\bar{\sigma}}(t) c_{\eta'k'\sigma}(t) | f_\sigma^\dagger b(t_1) \rangle \rangle^r.$$

Notice that all these next generation of GFs involve the excitation of two electrons in the electrodes. In what follow, we employ the well-known truncated scheme, the Lacroix's decoupling approximation (LDA) to contract pairs of same-spin lead-lead electron operators and pairs of same-spin dot-lead electron operators.⁶⁰

$$\begin{aligned} \langle \langle c_{\eta''k''\bar{\sigma}}^\dagger(t) c_{\eta'k'\bar{\sigma}}(t) b^\dagger f_\sigma(t) | f_\sigma^\dagger b(t_1) \rangle \rangle^\nu &\approx \langle c_{\eta''k''\bar{\sigma}}^\dagger c_{\eta'k'\bar{\sigma}}(t) \rangle G_\sigma^\nu(t, t_1), \\ \langle \langle f_{\bar{\sigma}}^\dagger b(t) c_{\eta'k'\bar{\sigma}}(t) c_{\eta''k''\sigma}(t) | f_\sigma^\dagger b(t_1) \rangle \rangle^\nu &\approx \langle f_{\bar{\sigma}}^\dagger b c_{\eta'k'\bar{\sigma}}(t) \rangle G_{\eta''k''\sigma,\sigma}^\nu(t, t_1), \\ \langle \langle c_{\eta''k''\bar{\sigma}}^\dagger(t) c_{\eta'k'\sigma}(t) b^\dagger f_{\bar{\sigma}}(t) | f_\sigma^\dagger b(t_1) \rangle \rangle^\nu &\approx -\langle c_{\eta''k''\bar{\sigma}}^\dagger b^\dagger f_{\bar{\sigma}}(t) \rangle G_{\eta'k'\sigma,\sigma}^\nu(t, t_1). \end{aligned}$$

Then the formal solutions of the second generation of GFs are

$$G_{\eta'k'\bar{\sigma},\sigma}^{\bar{\sigma}\sigma,r}(t, t_1) = -\langle f_{\bar{\sigma}}^\dagger b c_{\eta'k'\bar{\sigma}}(t_1) \rangle \tilde{g}_{\eta'k'\bar{\sigma}}^r(t, t_1) + \sum_{\eta''k''} \int dt_2 \tilde{g}_{\eta'k'\bar{\sigma}}^r(t, t_2) V_{\eta''k''\bar{\sigma}}(t_2) \langle c_{\eta''k''\bar{\sigma}}^\dagger c_{\eta'k'\bar{\sigma}}(t_2) \rangle G_\sigma^r(t_2, t_1) - \sum_{\eta''k''} \int dt_2 \tilde{g}_{\eta'k'\bar{\sigma}}^r(t, t_2) V_{\eta''k''\sigma}^*(t_2) \langle f_{\bar{\sigma}}^\dagger b c_{\eta'k'\bar{\sigma}}(t_2) \rangle G_{\eta''k''\sigma,\sigma}^r(t_2, t_1), \quad (44)$$

$$G_{\eta'k'\sigma,\sigma}^{\bar{\sigma}\bar{\sigma},r}(t, t_1) = -i \int dt_2 g_{\eta'k'\sigma}^r(t, t_2) I_{\bar{\sigma}}(t_2) G_{\eta'k'\sigma,\sigma}^r(t_2, t_1), \quad (45)$$

where $I_{\bar{\sigma}}(t) = \sum_{\eta} [\Pi_{\eta\bar{\sigma}}(t) + \Pi_{\eta\sigma}^\dagger(t)]$ is the spin-resolved current difference between the left and right leads, and the auxiliary two-time retarded function $\tilde{g}_{\eta k \bar{\sigma}}^r(t, t')$ is defined as

$$\left(i \frac{\partial}{\partial t} - \epsilon_{\eta k}(t) - \delta_{d\sigma}(t) \right) \tilde{g}_{\eta k \bar{\sigma}}^r(t, t') = \delta(t - t'), \quad (46)$$

with $\delta_{d\sigma}(t) = \epsilon_{d\sigma}(t) - \epsilon_{d\bar{\sigma}}(t)$. Inserting the two formal solutions into Eqs. (40) and (41) and after lengthy and cumbersome calculations, we can derive closed explicit expressions for the second-order ADMs, under this decoupling approximation,

$$\begin{aligned} \Omega_{\eta\sigma p, \eta'1}(t) &= -\frac{i}{4} \Gamma_{\eta'\sigma}^0 |u_{\eta'}(t)|^2 \Pi_{\eta\sigma p}(t) + \sum_{p'} u_{\eta'}^*(t) \int_{-\infty}^t dt_2 \left(\left\{ \Gamma_{\eta'\sigma}^0 \frac{R_{p'}}{\beta} u_{\eta'}(t_2) + \frac{i}{2} [\Gamma_\sigma(t_2) + \Gamma_{\bar{\sigma}}(t_2)] \Pi_{\eta'\sigma p'}^*(t_2) \right\} \right. \\ &\quad \left. \times \Pi_{\eta\sigma p}(t_2) - \Gamma_{\eta\sigma}^0 \frac{R_p}{\beta} u_\eta^*(t_2) \Pi_{\eta'\sigma p'}^*(t_2) \right) \exp \left\{ i \int_{t_2}^t d\tau [\chi_{\eta p}^+(\tau) - \chi_{\eta' p'}^-(\tau) - \delta_{d\sigma}(\tau)] \right\}, \quad (47) \end{aligned}$$

$$\Omega_{\eta\sigma p, \eta'2}(t) = 0. \quad (48)$$

Employing the two closed second-order ADMEs, we rewrite Eq. (39) as

$$i \frac{\partial}{\partial t} \Pi_{\eta\sigma p}(t) = u_{\eta}^*(t) \frac{R_p}{\beta} \Gamma_{\eta\sigma}^0 (\rho_{00} + \rho_{\sigma\sigma}) + \left[\epsilon_{d\sigma}(t) - \frac{i}{4} (2\Gamma_{\sigma}(t) + \Gamma_{\bar{\sigma}}(t)) - \chi_{\eta p}^+(t) \right] \Pi_{\eta\sigma p}(t) + \sum_{\eta'p'} u_{\eta'}^*(t) \Omega_{\eta\sigma p, \eta' \bar{\sigma} p'}(t), \quad (49)$$

and the EOM for the auxiliary mode expansion of the second-order ADME, $\Omega_{\eta\sigma p, \eta' \bar{\sigma} p'}(t)$, reads

$$i \frac{\partial}{\partial t} \Omega_{\eta\sigma p, \eta' \bar{\sigma} p'}(t) = i \left\{ \Gamma_{\eta' \bar{\sigma}}^0 \frac{R_{p'}}{\beta} u_{\eta'}(t) + \frac{i}{2} [\Gamma_{\sigma}(t) + \Gamma_{\bar{\sigma}}(t)] \Pi_{\eta' \bar{\sigma} p'}^*(t) \right\} \Pi_{\eta\sigma p}(t) - i \Gamma_{\eta\sigma}^0 \frac{R_p}{\beta} u_{\eta}^*(t) \Pi_{\eta' \bar{\sigma} p'}^*(t) - \left[\chi_{\eta p}^+(t) - \chi_{\eta' p'}^-(t) - \delta_{d\sigma}(t) \right] \Omega_{\eta\sigma p, \eta' \bar{\sigma} p'}(t). \quad (50)$$

The two explicit expressions, Eqs. (49) and (50), for the EOMs for the first- and second-order ADMEs, are the main results of this paper. The two equations adding Eqs. (15), (32), (34), together with the normalization relation Eq. (11), thereby constitute the closed set of differential equations. We call them the SOQREs. Solving these differential equations for a given initial condition, will provide a suitable description of transient dynamics of higher order correlated coherent tunneling through an interacting QD under an influence of arbitrary time varying potentials. It is interesting to notice that the dynamical equation (50) is nonlinear which is stemming from the on-site Coulomb interaction. While for the non-interacting QD, the corresponding equation is vanishing at the WBL as abovementioned or is linear provided that Lorentzian band width function is employed.

IV. STEADY-STATE SOLUTIONS

In this section, we analyze the time-independent transport using the SOQREs and compare with other methods.

A. Hubbard-I approximation

First we discuss the HIA. The steady-state solution for the current matrices can be easily obtained from Eq. (43)

$$\Pi_{\eta\sigma p} = - \frac{\frac{R_p}{\beta} \Gamma_{\eta\sigma}^0 (1 - \rho_{\bar{\sigma}\bar{\sigma}})}{\epsilon_{0\sigma} - \frac{i}{2} \Gamma_{\sigma} (1 - \rho_{\bar{\sigma}\bar{\sigma}}) - \chi_{\eta p}^+}. \quad (51)$$

with $\Gamma_{\sigma} = \Gamma_{L\sigma}^0 + \Gamma_{R\sigma}^0$. For spin symmetric case, we have,

$$\rho_{\uparrow\uparrow} = \rho_{\downarrow\downarrow} = \frac{1}{3} + \frac{4}{3\Gamma_{\sigma}} \sum_{\eta p} \Re \Pi_{\eta\sigma p}. \quad (52)$$

This is a self-consistent equation, giving occupation number $\rho_{\sigma\sigma}$ as a function of applied bias voltage. Then the current of, for example, the left lead can be calculated from Eq. (16) as

$$I_L = \frac{4\Gamma_{L\sigma}^0 \Gamma_{R\sigma}^0}{\beta \Gamma_{\sigma}} \sum_p R_p \Re \left[\frac{(1 - \rho_{\bar{\sigma}\bar{\sigma}})}{\epsilon_{0\sigma} - \frac{i}{2} \Gamma_{\sigma} (1 - \rho_{\bar{\sigma}\bar{\sigma}}) - \chi_{Lp}^+} - \frac{(1 - \rho_{\bar{\sigma}\bar{\sigma}})}{\epsilon_{0\sigma} - \frac{i}{2} \Gamma_{\sigma} (1 - \rho_{\bar{\sigma}\bar{\sigma}}) - \chi_{Rp}^+} \right]. \quad (53)$$

On the other hand, according to the NGF approach developed by Meir and Wingreen, the electron occupation number is determined by solving the integral equation of the form⁶¹

$$\rho_{\sigma\sigma} = \int \frac{d\varepsilon}{\pi} \frac{\Gamma_{L\sigma}^0 f_L(\varepsilon) + \Gamma_{R\sigma}^0 f_R(\varepsilon)}{\Gamma_{\sigma}} \Im G_{\sigma}^r(\varepsilon), \quad (54)$$

and the current for an interacting QD is expressed by the generalized Landauer formula

$$I_L = - \int d\varepsilon \frac{4\Gamma_{L\sigma}^0 \Gamma_{R\sigma}^0}{\Gamma_{\sigma}} [f_L(\varepsilon) - f_R(\varepsilon)] \Im G_{\sigma}^r(\varepsilon). \quad (55)$$

Employing the analytic expression for the retarded GF under HIA of the central region, Eq. (42), and the Pádé decomposition of the Fermi function, Eq. (27), one can easily evaluate the occupation number $\rho_{\sigma\sigma}$ and the current I_L , which is found to be in exact agreement with the SOQRE results, Eqs. (52) and (53).

B. Simplified Lacroix's decoupling approximation

Since the SOQRE Eq. (50) is a nonlinear equation, we can not obtain a simple analytical steady-state solution. About twenty years ago, Meir *et al.* developed a simplified version of the LDA (SLDA) in the EOM method of the retarded GF to investigate electron tunneling through a QD out of equilibrium and/or in the presence of a magnetic field.⁶¹ This SLDA produces interesting results for the bias voltage dependence of the differential conductance, showing a zero-bias anomaly and peak splitting due to Zeeman effect in the presence of a magnetic field. This approximation has been believed to provide qualitatively correct description for the Kondo-type electronic transport through a QD when the temperature is higher than the Kondo temperature, $T \geq T_K$. In their approximation, Meir *et al.* derived the analytical solution of the second retarded GF $G_{\eta'k'\sigma}^{\sigma\sigma,r}(t, t_1)$ to the order of $V_{\eta k\sigma}^2$, by simplifying Eq. (44): neglecting the inhomogeneous term involving tunneling and ignoring the back action of the electron tunneling on the electron distributions of electrodes, i.e., $\langle f_{\bar{\sigma}}^{\dagger} b c_{\eta'k'\bar{\sigma}} \rangle \approx 0$, $\langle c_{\eta''k''\bar{\sigma}}^{\dagger} c_{\eta'k'\bar{\sigma}} \rangle \approx \delta_{\eta''\eta'} \delta_{k''k'} f_{\eta'}(\epsilon_{\eta'k'})$.⁶¹ At the end, we find that the EOM for the second-order ADME, $\Omega_{\eta\sigma p, \eta' \bar{\sigma} p'}(t)$, Eq. (50) becomes a linear differential equation,

$$i \frac{\partial}{\partial t} \Omega_{\eta\sigma p, \eta' \bar{\sigma} p'}(t) = i \Gamma_{\eta' \bar{\sigma}}^0 \frac{R_{p'}}{\beta} u_{\eta'}(t) \Pi_{\eta\sigma p}(t)$$

$$-\left[\chi_{\eta p}^+(t) - \chi_{\eta' p'}^-(t) - \delta_{d\sigma}(t)\right] \Omega_{\eta\sigma p, \eta'\sigma p'}(t). \quad (56)$$

Besides, under this approximation, an analytical expression for the retarded GF can be derived in the frequency domain as

$$G_{\sigma}^r(\varepsilon) = \frac{1 - \rho_{\bar{\sigma}\bar{\sigma}}}{\varepsilon - \epsilon_{0\sigma} - \Sigma_{0\sigma}^r - \Sigma_{1\sigma}^r(\varepsilon)}, \quad (57)$$

with $\Sigma_{0\sigma}^r = -i(\Gamma_{L\sigma}^0 + \Gamma_{R\sigma}^0)/2$, and

$$\Sigma_{1\sigma}^r(\varepsilon) = \sum_{\eta k} |V_{\eta k}^0|^2 \frac{f_{\eta}(\epsilon_{\eta k}^0)}{\varepsilon - \epsilon_{\eta k}^0 + i0^+}. \quad (58)$$

Since the current formula Eq. (55) is general, we can still use it to evaluate the current through an interacting QD in the SLDA provided that the retarded GF is replaced by Eq. (57). While the SOvN approach gives a quite different current⁴⁶

$$I_L = - \int d\varepsilon \frac{2\Gamma_{L\sigma}^0 \Gamma_{R\sigma}^0}{|\varepsilon - \epsilon_{0\sigma} - \Sigma_{0\sigma}^r - \Sigma_{1\sigma}^r(\varepsilon)|^2} [f_L(\varepsilon) - f_R(\varepsilon)]. \quad (59)$$

The difference, we believe, is coming from the fact that the GF method is a double-time dynamical theory, while the SOvN is a single-time theory. We emphasize that our SOQRE is based on the GF method.

C. Numerical discussions

In what follows we perform numerical calculations based on the SOQREs with both the LDA and SLDA for the steady-state transport in absence of magnetic field. In the calculations, we only consider the symmetric system, $\Gamma_{L\sigma}^0 = \Gamma_{R\sigma}^0 = \frac{1}{2}\Gamma$, and use Γ as energy unit throughout this paper. Moreover, we assume that the external bias voltage is applied only to the left lead, $\mu_L = eV$, while the chemical potential of the right lead remains unchanged, $\mu_R = 0$.

To demonstrate the strong electron correlation effect on tunneling, we set that the energy level of the QD lies at least a resonance width Γ below the chemical potentials of the leads at equilibrium. To be specific, we choose, in the following calculations, $\epsilon_d = -2\Gamma$. Therefore, this QD will show the Kondo effect, i.e., a peak at the Fermi energy in the equilibrium density of states (DOS), $\rho_d(\omega = 0)$, of the dot electrons, when the temperature becomes lower than a typical energy scale, the Kondo temperature defined as $T_K = \sqrt{W\Gamma/4} \exp(-\pi |\epsilon_d|/\Gamma)$, where W is a high-energy cutoff equal to the half bandwidth. Here we set the half bandwidth $W = 20\Gamma$, leading to the Kondo temperature $T_K = 0.0042\Gamma$ for this QD. It is well-known that for the lead-QD-lead system, the bias-voltage-dependent differential conductance is proportional to the equilibrium spectral density of the dot electrons at nearly zero temperature. Then we first analyze the current-voltage characteristic of the system at

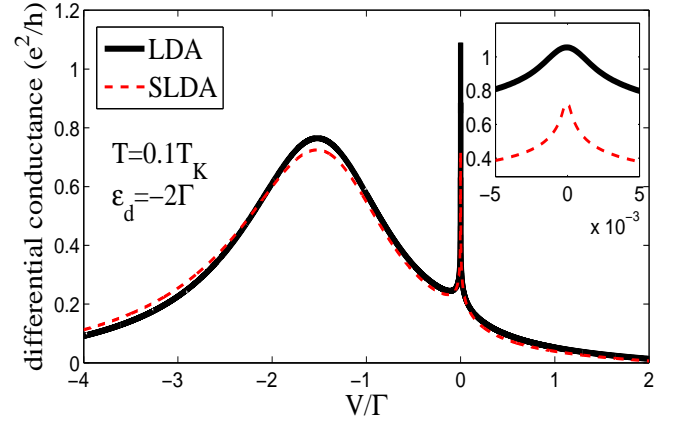


Figure 1: (Colour online) The calculated steady-state differential conductance vs the applied bias voltage under $\mu_L = V$, $\mu_R = 0$ in the SOQRE theory with LDA (solid line) and SLDA (dashed line), respectively, for the system with $\epsilon_d = -2\Gamma$ at the temperature $T = 0.1T_K$. Inset: the detailed behavior of the Kondo peak around $V = 0$.

the temperature $T = 0.1T_K$ and plot the calculated differential conductance in Fig. 1. The numerical results present two clear peaks in the DOS of the QD: a wide peak located nearly at $V = -2\Gamma$ corresponds to the single-particle state of the QD, and an extremely sharp peak located exactly at $V = 0$ is stemming from the strongly correlated state at the Fermi energy, i.e., the Kondo peak. Furthermore, we find that the LDA gives the $\rho_d(\omega = 0) \simeq 1.05$ at $T = 0.1T_K$, which is in perfect agreement with the recent analytical calculations based on the exact EOM solutions for the impurity's retarded GF under the same approximation.⁶³ This value is fifty percent larger than the SLDA's, as shown in the inset of Fig. 1.

To get further comparison between the two approximations, we investigate the temperature dependences of the two-terminal linear conductances in a wide temperature range, from $T = 10^{-4}\Gamma$ to 10Γ , as shown in Fig. 2. The linear conductance can be calculated by expanding the SOQREs to the first order with respect to the bias voltage V in the limit of $V \rightarrow 0$. It is clear to observe that the conductance of the LDA increases gradually with decreasing of temperature up to nearly $1.2e^2/h$ at $T = 10^{-4}\Gamma = 0.025T_K$, which is also consistent with the exact EOM solutions.⁶³ Instead, the conductance of the SLDA exhibits an obvious decrease when the temperature becomes lower than the Kondo temperature. These results indicate that taking full account of the inhomogeneous tunneling term and the back action effect on the electrodes is necessary in order to obtain qualitatively correct description of the Kondo-type transport through a QD at $T < T_K$. Therefore, we can conclude that the present SOQRE approach is an appropriate theoretical formulation to investigate the electronic tunneling in the Kondo regime and constitutes a very practical starting point for the investigation of transient Kondo dynamics.

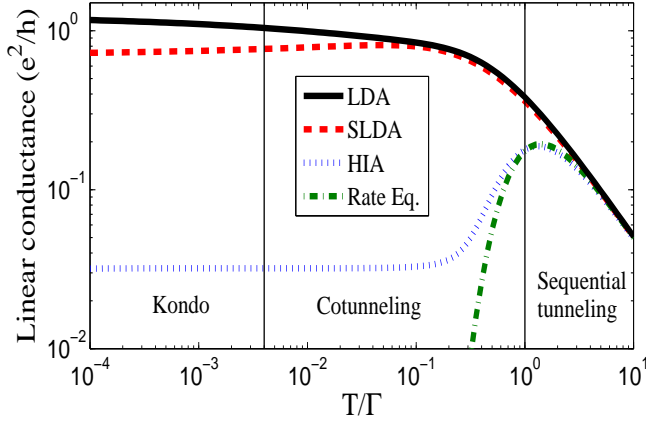


Figure 2: (Colour online) The linear conductance as a function of the temperature T/Γ varying from 10^{-4} to 10 for the system with $\epsilon_d = -2\Gamma$. We show the calculated results by the SOQREs with three different approximations, LDA (solid line), SLDA (dashed line), and HIA (dashed-dotted line). For comparison, we also plot the result of the first-order rate equation (dotted line).

On the contrary, the conductances of the two approximations are getting closer when the temperature is higher than the Kondo temperature, $T > T_K$, and becomes nearly indistinguishable at $T > 0.1\Gamma$. For comparison, we also plot the linear conductances calculated by the HIA and the first-order rate equation^{43,44} (FORE, i.e., the lowest non-vanishing order in the tunneling-coupling strength Γ) in Fig. 2. It is found that the HIA and the FORE are completely failure in describing electronic correlated tunneling through an interacting QD when the temperature is decreased to values of the order of the tunneling-coupling strength or lower, $T < \Gamma$. In the context of quantum transport in nanoscale system, it is well-known that the FORE is only valid when the temperature is higher than the tunneling strength, i.e., $T > \Gamma$, at which the sequential tunneling is the dominated tunneling mechanism.^{39,42,43} We observe actually here that the results of the HIA and the FORE are accurately equal to those of the SOQREs at $T \geq 2\Gamma$, since the adequately strong thermal-broadening induces the occurrence of resonant-tunneling. From this figure, we can therefore classify the electronic tunneling through a single QD system into three different physical scenarios depending on the temperature: (1) At low temperatures, $T \leq T_K$, the strongly correlated Kondo singlet state is formed and plays a critical role in tunneling, leading to a great enhancement of the linear conductance. This regime is the well-known Kondo regime;^{61–64} (2) At the intermediate region, $T_K < T < \Gamma$, an obvious enhancement of the linear conductance is still observed even though the Kondo resonance is not formed. As discussed above, at this region of temperatures, the tunneling processes of higher order in Γ involving two or more electrons play crucial role, which is called electron correlated tunneling (i.e., cotunneling) in literature.^{39,45,46}

The enhancement of conductance is ascribed to the renormalization effects of dot level due to coupling to the electrodes. It is reminiscence of the strong correlation effect; (3) At high temperatures, $T \geq \Gamma$, the QD system is in the sequential tunneling regime.

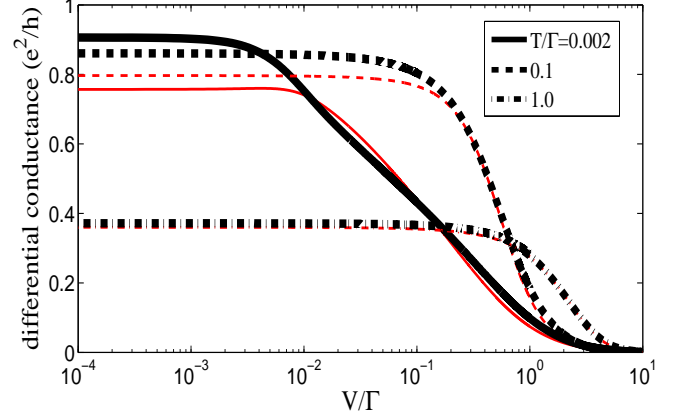


Figure 3: (Colour online) The differential conductance as a function of the bias voltage for the system with $\epsilon_d = -2\Gamma$ at three different temperatures, $T/\Gamma = 0.002$ (solid lines), 0.1 (dashed lines), and 1.0 (dashed-dotted lines), calculated by the SOQREs with the LDA (thick-black lines) and SLDA (thin-red lines).

Finally, we investigate the differential conductance as a function of bias voltage at different temperatures, as shown in Fig. 3. It is found that the unambiguous difference between the two approximations disappears with increasing bias voltage due to the decoherence effect introduced by nonequilibrium.

V. TRANSIENT DYNAMICS

In this section, we perform numerical investigations on the spin-independent transient response of the interacting QD under various time-varying bias voltages, including steplike and harmonic modulations, by using a fourth-order Runge-Kutta scheme to solve the ensuing SOQREs. Therefore, we have to propagate every spin-independent second-order ADME, $\Omega_{\eta p, \eta' p'}(t)$, with time, which contains totally $8N_p^2$ unknown real quantities to propagate. The memory requirement of the proposed method scales with $N_M = 8N_p^2 + 4N_p + 1$ and the computational time requirement scales with $N_T \times N_M$ (N_T is the number of time steps). Notice that for lower temperature, more Padé pole pairs need to be considered in the Padé spectrum decomposition of the Fermi function to ensure the numerical convergence. In the following calculations, we will hence focus our attention on the transient current only at an intermediate temperature, $T = 0.1\Gamma$, for the purpose of avoiding huge computational burden. It deserves to point out that since the main tunneling mechanism is the cotunneling at this temperature as discussed above, our following simulations provide us a

cheap and reasonable benchmark for understanding the strong correlated effects on electronic transient tunneling through nanoscale systems. Besides, it is indicated in Figs. 2 and 3 that the SLDA is sufficiently accurate at this temperature. Then we will employ this approximation in the time evolution calculations.

A. Response to steplike modulation

In this subsection, we investigate the response of the interacting QD system to a large rectangular pulse bias potential of duration s . We assume that the chemical potentials of both leads are zero initially, and at $t = 0$, a bias pulse with amplitude Δ_L is suddenly applied to the left lead, and increases the single-level energy of the QD by Δ_d , but leaves the right lead unbiased. At a later time $t = s$ the pulse is switched off. This means following time dependences:

$$\begin{aligned}\epsilon_{d\sigma}(t) &= \epsilon_d + [\theta(t) - \theta(t-s)]\Delta_d, \\ \Delta_L(t) &= [\theta(t) - \theta(t-s)]\Delta_L, \\ \Delta_R(t) &= 0.\end{aligned}$$

We further assume that the barrier heights do not depend on time, i.e., $u_n(t) \equiv 1$.

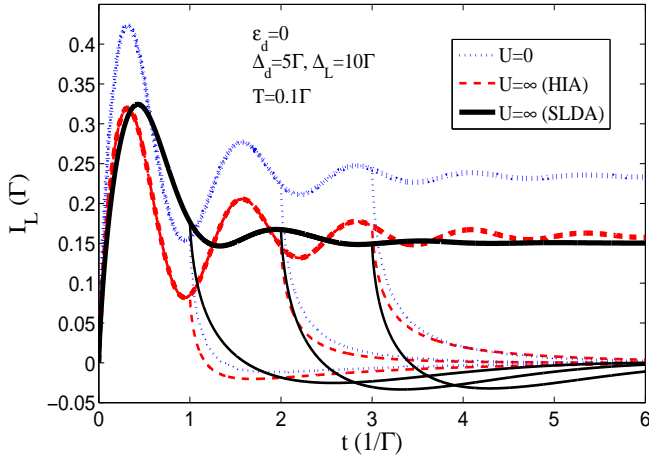


Figure 4: (Colour online) Time-dependent current $I_L(t)$ through left lead in response to an upward step pulse with different durations $s = \infty, 3/\Gamma, 2/\Gamma$, and $1/\Gamma$, for the system with $\epsilon_d = 0$ at the temperature $T = 0.1\Gamma$ by the SOAREs with the SLDA (black-solid line) and the HIA (red-dashed line). In comparison, we also plot the results of a noninteracting single-level QD with the SOQREs (blue-dotted line).

In order to compare with the previous relevant work of exact EOM solutions, we first compute the current responses to step pulses with several durations for both the noninteracting single-level QD ($U = 0$) and the interacting QD ($U = \infty$) with the same energy level $\epsilon_d = 0$ at the temperature $T = 0.1\Gamma$. The calculated time evolutions of current are plotted in Fig. 4 for the parameters: $\Delta_L = 10\Gamma$ and $\Delta_d = 5\Gamma$. It is clear that the simulations for the noninteracting system exactly recover the

previous results of exact EOM solutions:^{17,20} a ringing in the response current as a result of coherent electronic transitions between the leads and the QD with a pulse-amplitude-dependent period¹⁷

$$\Delta t_L = \frac{2\pi\hbar}{|\Delta_L - (\epsilon_d + \Delta_d)|}. \quad (60)$$

For the interacting system the current with the HIA behaves similarly as the noninteracting system, exhibiting ringing with the same period $\Delta t_L = 1.26/\Gamma$, but with an overall reduced amplitude. Nevertheless, the current response changes greatly if the correlation effect is considered more rigorously with the SLDA as shown by the black-solid line in Fig. 4. It is found, such as, that the oscillation period is altered due to the level renormalization of the QD by the two-electron correlation tunneling as analyzed in the following discussions; the response time of the first peak is slower because the repulsive Coulomb interaction inhibits electron motion through the QD; the ringing fades away more quickly, which is a consequence of account of the bias-voltage-induced decoherence effect within the SLDA; and a temporary sign reversal of current is shown immediately after the pulse ends, which is absent in the HIA and noninteracting cases.

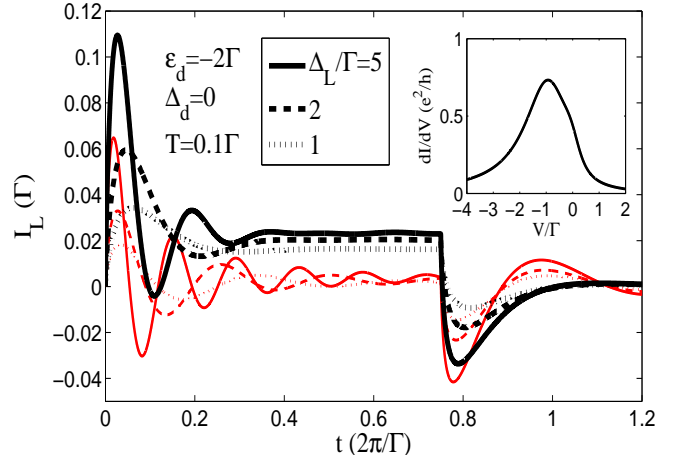


Figure 5: (Colour online) Time-dependent current $I_L(t)$ through left lead in response to an upward step pulse of the duration $s = 1.5\pi/\Gamma$ for the system with $\epsilon_d = -2\Gamma$ by the SLDA (black lines) and HIA (red lines). The current is driven by different applied bias voltages: $\Delta_L/\Gamma = 5$ (solid lines), 2 (dashed lines), and 1 (dotted lines). The other parameters: $\Delta_d = 0$, $T = 0.1\Gamma$. Inset: The corresponding differential conductance calculated by the SOQREs with SLDA is plotted as a function of bias voltage in the case of steady-state transport.

In Fig. 5, we study the current response behavior in the case that the energy of the QD level always remains at the Kondo regime, $\epsilon_d = -2\Gamma$, even as the bias pulse is applied (i.e. $\Delta_d = 0$), to analyze further the effect of correlation on transient dynamics. It is clear that the HIA calculations predict the same period of current oscillation as indicated by Eq. (60), for example, $\Delta t_L = 2\pi/7\Gamma$ for the case of $\Delta_L = 5\Gamma$, nevertheless

the SLDA calculations show that the current oscillates with a different period $\Delta t_L = 2\pi/6\Gamma$. The SLDA calculation also disagrees with the time-dependent NCA calculation, which predicts that the ringing period is independent of dot level ϵ_d , but instead is dependent only on the bias voltage, $2\pi/\Delta_L$.³⁰ This specific period has been ascribed to the Kondo peak splitting. The nonequilibrium DOS of the Kondo dot exhibits the splitting of the Kondo peak into two resonances, one at the Fermi energy of each lead. The coherent electronic transitions between the two peaks induce current oscillation with a period $2\pi\hbar/|\mu_L + \Delta_L - \mu_R - \Delta_R| = 2\pi/\Delta_L$.³⁰ However, since we consider the temperature $T = 0.1\Gamma$ being much higher than the corresponding Kondo temperature, $T_K = 0.0042\Gamma$, no Kondo peak appears in the equilibrium DOS of the dot electrons, as clearly shown in the inset of Fig. 5. Interestingly, a wide peak is found nearly at $V = -1.0\Gamma$, which indicates that two-electron correlated tunneling causes an obvious renormalization, $\tilde{\epsilon}_d \simeq -1.0\Gamma$, of the single-particle energy level of the dot. As far as this level renormalization is concerned, we can still ascribe our new ringing period to coherent electronic transitions between the leads and the QD with the renormalized level, that is

$$\Delta t_L = \frac{2\pi\hbar}{|\Delta_L - (\tilde{\epsilon}_d + \Delta_d)|}. \quad (61)$$

B. Response to harmonic modulation

Now we move to investigate another time-dependent transport when external bias voltage is periodic in time. To be specific, we assume that the ac bias voltages is applied in-phase to the leads and dot as

$$\Delta_{d,\eta}(t) = \Delta_{d,\eta} \cos(\omega_{ac}t). \quad (62)$$

Figure 6 exhibits the time evolutions of current under harmonic bias voltages with various driving amplitudes Δ_L superposed to a dc bias voltage V at the temperature $T = 0.1\Gamma$. At the case of high dc bias voltage, $V = 5.0\Gamma$, the response current shows the rich structure as displayed in Fig. 6(a) that many harmonics are excited except for the case of low driving amplitude $\Delta_L = V/10 = 0.5\Gamma$. At the linear transport regime, the current response is different from that at the nonlinear regime. For instance, Fig. 6(b) shows that only the dc and the first harmonic are enhanced in the current response at the case of low dc bias voltage, $V = 0.2\Gamma$, even subject to a relatively strong driving voltage up to $\Delta_L = 5V = 1.0\Gamma$. This conclusion can be further confirmed by numerical calculation of the Fourier spectrum of the time-dependent current. We display the corresponding spectrum analysis (the ratio of amplitude of the n th harmonic component of the current, I_n , to the dc part, I_0) in Fig. 7 for the two cases. The current response to a harmonic modulation was previously studied for the Kondo model based on the Schrieffer-Wolff unitary transformation by

means of bosonization method at the Toulouse limit and perturbation theory, respectively.^{24,25} The two analytical solutions for the ac Kondo model predicted controversial results on the transient current spectrum. The present investigation provides current spectrum behavior that is different from both previous results. From Fig. 7, we can state that at temperatures above the Kondo temperature, the magnitudes of the dc and ac components are governed by two independent parameters, the dc bias voltage V and the driving voltage Δ_L ; the first harmonic component has a similar magnitude as the dc component and has at least one order of stronger magnitude than higher harmonics at the linear dc transport regime [Fig. 7(b)]; while the second and even several higher harmonics are equally enhanced as the first harmonic component at the nonlinear dc transport regime [Fig. 7(a)]. Therefore, our results show that the response current in the cotunneling regime has similar frequency spectrum behavior as the noninteracting system (of course the current is largely enhanced by the electron correlation effect).

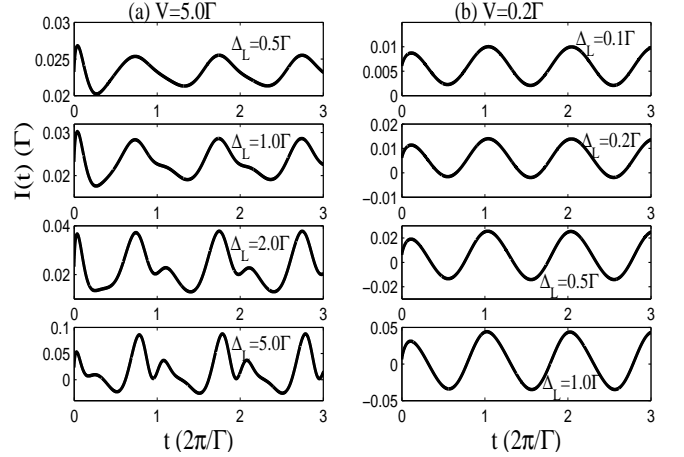


Figure 6: (Colour online) The time evolutions of the current for harmonic modulations with different driving voltages Δ_L for two dc bias voltages, $V = 5\Gamma$ (a) and 0.2Γ (b). The other parameters: $\epsilon_d = -2\Gamma$, $T = 0.1\Gamma$, $\Delta_d = \Delta_R = 0$. The modulation frequency is $\omega_{ac} = 3\Gamma$.

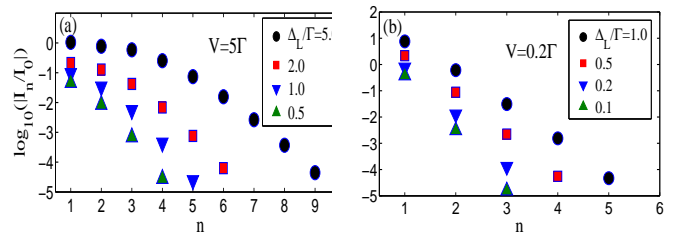


Figure 7: (Colour online) The Fourier representations of the current with different driving voltages Δ_L for two dc bias voltages, $V = 5\Gamma$ (a) and 0.2Γ (b). The other parameters are the same as those in Fig. 6.

In experiments, an easily measurable quantity is the dc differential conductance, which exhibits the famous zero-

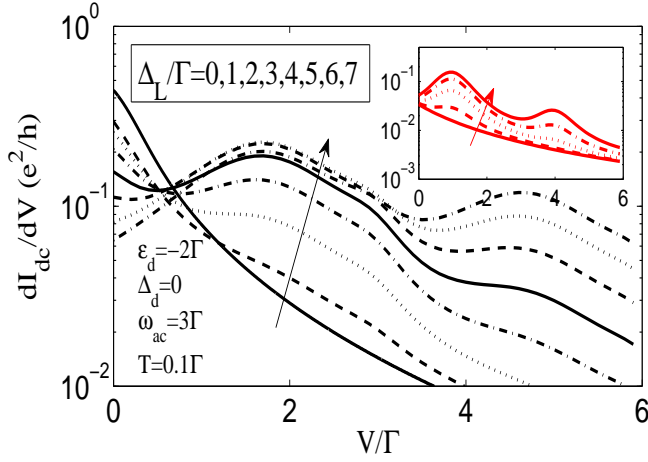


Figure 8: (Colour online) The calculated dc differential conductance dI_{dc}/dV versus dc bias voltage V subject to a harmonic modulation with the frequency $\omega_{ac} = 3\Gamma$ and various amplitudes Δ_L for the system with $\epsilon_d = -2\Gamma$ at the temperature $T = 0.1\Gamma$. The other parameters: $\Delta_d = \Delta_R = 0$. Inset: The corresponding results of the noninteracting QD.

bias anomaly as one of the hallmarks of the nonlinear Kondo effect and electron correlated tunneling (Fig. 3). In the presence of strong ac modulation, the dc differential conductance, defined as the derivative of time-average current I_{dc} with respect to dc bias voltage V , will exhibit side peaks with increasing dc bias voltage that is ascribed to the photon absorption assisted tunneling, as shown in Fig. 8, in which we plot the dc dI_{dc}/dV versus dc bias voltage at different amplitudes of the driving field. At a sufficiently large modulation frequency, the noninteracting QD has resonances at $V = \epsilon_d + n\hbar\omega_{ac}$ (see the inset of Fig. 8), while the previous analytical solutions for the Kondo model suggested different characteristic resonances located at $V = n\hbar\omega_{ac}$ resulted from the splitting of the Kondo peak in the nonequilibrium situation.^{24,25} However, we can see clearly from Fig. 8 that at the temperature where the cotunneling dominates, the resonances occur at different locations, $V = \epsilon_d + n\hbar\omega_{ac}$, due to the electron correlation induced level renormalization as indicated in the above subsection, if the driving field is sufficiently strong. Besides, in contrast to the noninteracting system, the zero-bias anomaly is suppressed by the harmonic modulation, even leading to a zero-bias minimum.²⁵⁻²⁷

C. Linear response

Another important issue in the context of the time-dependent transport in nanoscale devices is the current response to a small ac voltage driving, which is applied across the central region in addition to a dc bias voltage, i.e., the linear ac conductance in a nonequilibrium situation for particularly the interacting systems. The present SOQREs facilitate the calculation of the current

response in the limiting case of a slight ac amplitude, $\Delta_L(t) = -\Delta_R(t) = \frac{1}{2}\delta V \cos(\omega t)$ with $\delta V \rightarrow 0$.

For the sake of convenience, we rewrite the SOQREs with SLDA in matrix form:

$$\frac{\partial \mathbf{q}}{\partial t} = [\mathbf{A}_0 + \mathbf{A}_1 \delta V \cos(\omega t)] \mathbf{q} + \mathbf{B}, \quad (63)$$

where $\mathbf{q} = (\rho_{\sigma\sigma}, \Pi_{\eta\sigma p}, \Pi_{\eta\sigma p}^\dagger, \Omega_{\eta\sigma p}, \eta' \bar{\sigma} p', \Omega_{\eta\sigma p}^\dagger, \eta' \bar{\sigma} p')^T$ and the matrices \mathbf{A}_0 , \mathbf{A}_1 , and \mathbf{B} can be read from Eqs. (15), (49), and (56). Under the condition of small oscillation amplitude, the time-dependent ADMEs \mathbf{q} can be expanded as⁴⁴

$$\mathbf{q} = \mathbf{q}^{(0)} + (\mathbf{q}^{(11)} e^{i\omega t} + \mathbf{q}^{(1\bar{1})} e^{-i\omega t}) \delta V, \quad (64)$$

where $\mathbf{q}^{(0)}$ represents the zeroth order solution irrespective of the ac field, i.e., the stationary solution without ac modulation, and $\mathbf{q}^{(1\pm 1)}$ is the positive (negative) frequency part of the first order correction to the stationary solution. Substituting this expansion into the time-dependent SOQREs Eq. (63) and expanding according to the perturbation parameter δV , therefore, we obtain⁴⁴

$$\mathbf{q}^{(0)} = -\mathbf{A}_0^{-1} \mathbf{B}, \quad (65)$$

$$\mathbf{q}^{(1\pm 1)} = (\pm i\omega \mathbf{I} - \mathbf{A}_0)^{-1} \mathbf{A}_1 \mathbf{q}^{(0)}, \quad (66)$$

with \mathbf{I} being the unit matrix. Using the first order correction term $\mathbf{q}^{(1\pm 1)}$ we can calculate the linear response current as

$$\begin{aligned} \delta I_{\eta\sigma}(t) = & \left\{ -\frac{3}{2} \Gamma_{\eta\sigma} \rho_{\sigma\sigma}^{11} + \sum_p \left[\Pi_{\eta\sigma p}^{11} + (\Pi_{\eta\sigma p}^{11})^* \right] \right\} e^{i\omega t} \delta V \\ & + \left\{ -\frac{3}{2} \Gamma_{\eta\sigma} \rho_{\sigma\sigma}^{1\bar{1}} + \sum_p \left[\Pi_{\eta\sigma p}^{1\bar{1}} + (\Pi_{\eta\sigma p}^{11})^* \right] \right\} e^{-i\omega t} \delta V. \end{aligned} \quad (67)$$

Then we perform Fourier transformation of the total current $\delta I(t) = \sum_\sigma (\delta I_{L\sigma} + \delta I_{R\sigma})/2$ and obtain the linear response admittance $G(\omega)$ of the QD

$$G(\omega) = \frac{\delta I(\omega)}{\delta V}. \quad (68)$$

In Fig. 9 we show the resulting linear response admittance $G(\omega)$ at the linear transport ($V = 0$) and nonlinear transport (a finite dc bias voltage $V \neq 0$ is applied symmetrically between the left and right leads, i.e., $\mu_L = -\mu_R = V/2$) regimes. Note that our sign of the imaginary part of the admittance is opposite to the sign in Ref. 71 and that a positive (negative) $\Im G(\omega)$ corresponds to the sign of a capacitive (inductive) component. For zero external dc bias voltage, the calculated admittance for the noninteracting system resembles exactly the results reported by Fu and Dudley:⁷¹ For the QD with $\epsilon_d = -2\Gamma$, the admittance is capacitive at low frequencies, but turns to an inductive behavior at $\omega \sim |\epsilon_d|$, meanwhile the ac conductance $g(\omega) = \Re G(\omega)$ exhibits a peak implying that a photon-assisted resonance is satisfied at this condition. Moreover, present investigation shows that a finite dc bias voltage will change the

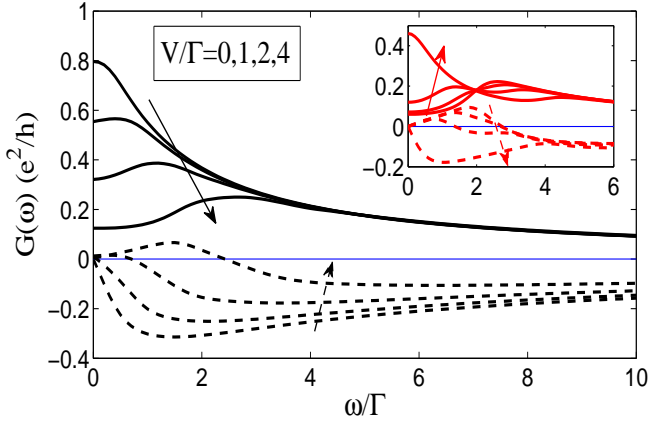


Figure 9: (Colour online) Real $\Re G(\omega)$ (solid lines) and imaginary $\Im G(\omega)$ (dashed lines) parts of the linear response admittance, $G(\omega)$, versus frequency for different dc bias voltages V for the QD with $\epsilon_d = -2\Gamma$ at the temperature $T = 0.1\Gamma$. Inset: The corresponding results for the noninteracting system.

crossover point as $\omega \sim |\epsilon_d - \mu_R| = |\epsilon_d + V/2|$ since a new photon-assisted resonance is formed between the level and the right lead. At the case of $V = 4\Gamma$, the admittance becomes always inductive behavior and a monotonically decreasing of the ac conductance. It is nevertheless observed that the bias voltage dependence of the admittance exhibits contrary behavior for the interacting QD in the cotunneling regime. The external bias voltage induces suppression of the ac conductance at low frequencies. The equilibrium admittance is always inductive but becomes capacitive at low frequencies due to external dc bias driving. Therefore, we can conclude that the correlation effect greatly changes the linear ac-response behavior of the QD.

VI. CONCLUSION

In this paper, we have presented a convenient approach for the time-dependent electronic Kondo-type tunneling and cotunneling through an interacting QD subject to arbitrary time-varying potentials based on the TDNGF. For this purpose, we have followed the theoretical strategy of a recently developed propagation scheme for time-dependent transport in a noninteracting QD, in which a set of coupled ordinary differential equation with only one time argument is derived based on the double-time TDNGF by the help of an auxiliary-mode expansion.⁵⁴ Unlike the case of noninteracting QD, the second-order ADMEs of the interacting system are however found to be related to the two-particle GFs, whose EOMs will inevitably generate the next-order GFs due to the on-site Coulomb interaction. Then we have employed the famous LDA and its simplified version to evaluate the higher order GFs. At the end, a closed set of coupled single-time evolution equations called SOQREs has been established. It deserves to notice that, in comparison with the previ-

ous SOvN approach, the SOQREs can provide correct description for transient dynamics of the correlated electron transport, since no Markov approximation is invoked in its derivation. Meanwhile, the SOQREs deal with the electron correlation more rigorously because this scheme is closely joint with the NGF technique, which is believed to be most powerful method to investigate the strongly electronic correlation effect.

To validate the present approach, we have first utilized the resulting differential equations to investigate the steady-state transport. Our numerical calculations show that the SOQREs with the original LDA is valid at the whole range of temperature, from the Kondo-type tunneling regime to the sequential tunneling regime, while the SOQREs with the SLDA is only valid at temperatures above the Kondo temperature since this simplified decoupling approximation takes no account of the back action effect of electron tunneling on the electrodes.

As applications, we have employed the present SOQREs with the SLDA to investigate time-dependent cotunneling through an interacting QD in response to abrupt change and a harmonic modulation of bias voltage, respectively. Our calculations have revealed some new interesting physics in the current response behavior: 1) a ringing of current with a new period after a sharp bias turn-on; 2) similar frequency spectrum response of the ac-driving current with the noninteracting QD; but 3) different time-average current-dc bias voltage characteristic from the noninteracting QD, such as suppression of zero-bias peak in the dc differential conductance with increasing harmonic modulation amplitude and a new photon-assisted resonant condition. Our further analysis has indicated that these features are ascribed to an effective renormalization of the dot level due to the interplay of electron correlation and coherent tunneling between the QD and leads. Finally, we have discussed ac linear-response at arbitrary dc bias voltage and predicted that the interacting QD exhibits entirely different linear-response admittance from the noninteracting system.

Before ending this paper, let us mention a few possible directions of future research. First, a WBL has been invoked in the derivation of the SOQREs in the present work. Such model has a great advantage that it is very easy for theoretical calculation and can still provide some insight into the physics of time-dependent transport through a QD, even though it is far from a realistic device. The present formulation, nevertheless, can be readily extended to the case of a finite bandwidth, such as the Lorentzian linewidth. Moreover, it is known that the electronic spectral density inside the QD satisfies the Fermi liquid unitary limit $\rho_d(\omega = 0) = 2/\Gamma$ (This DOS implies that the linear conductance reaches its unitary limit, $2e^2/h$.) when the temperature goes to zero.⁶²⁻⁶⁴ However, the present approach can not reach such unitary limit since the LDA results in a logarithmic- T dependence of the DOS in the low- T limit but not the exact T^2 dependence.^{62,63} Therefore, the third-order quantum rate equations approach based on a more rigorous decou-

pling approximation beyond the LDA,⁶⁴ is desirable for future investigation of time-dependent Kondo physics at extremely low temperature.

Acknowledgments

This work was supported by Projects of the National Basic Research Program of China (973 Program) under Grant No. 2011CB925603, and the National Science Foundation of China, Specialized Research Fund for the Doctoral Program of Higher Education (SRFDP) of China.

Appendix: Padé expansion of the Fermi function

In order to perform the energy integration in the self-energies Eqs. (21) and (22), it is needed to expand the Fermi function in terms of a finite sum over simple poles. The Padé spectrum decomposition is believed to be most efficient in numerical calculation, which is defined as follows:^{57,69,70}

$$f(x) = \frac{1}{1 + e^x} = \frac{1}{2} - \frac{1}{2} \frac{\sinh(x/2)}{\cosh(x/2)}$$

$$\approx \frac{1}{2} - \sum_{p=1}^{N_p} R_p \left(\frac{1}{x - i\chi_p} + \frac{1}{x + i\chi_p} \right), \quad (\text{A.1})$$

where R_p is the p th residue in the Padé expansion, $i\chi_p$ ($\chi_p > 0$) is the p th Padé pole in the upper complex plane, and N_p is the number of Padé pole pairs. For this decomposition, the residues and poles can be given by the eigenvalue problem of the symmetric matrix B ,⁶⁹

$$B |b_p\rangle = b_p |b_p\rangle, \quad (\text{A.2})$$

with

$$B_{n,n+1} = \frac{1}{2\sqrt{(2n-1)(2n+1)}}, \quad n \geq 1, \quad (\text{A.3})$$

as

$$\chi_p = 1/b_p, \quad (\text{A.4})$$

$$R_p = |\langle 1 | b_p \rangle|^2 / (4b_p^2). \quad (\text{A.5})$$

-
- ¹ T. Fujisawa, T. Hayashi, and S. Sasaki, Rep. Prog. Phys. **69**, 759 (2006).
 - ² J.P. Pekola, O.-P. Saira, V.F. Maisi, A. Kemppinen, M. Möttönen, Y.A. Pashkin, D.V. Averin, Rev. Mod. Phys. **85**, 1421 (2013).
 - ³ J. Gabelli, G. Fève, J.M. Berroir, B. Plaças, A. Cavanna, B. Etienne, Y. Jin, and D.C. Glattli, Science **313**, 499 (2006).
 - ⁴ G. Fève, A. Mahé, J.M. Berroir, T. Kontos, B. Plaças, D.C. Glattli, A. Cavanna, B. Etienne, and Y. Jin, Science **316**, 1169 (2007).
 - ⁵ M. Switkes, C.M. Marcus, K. Campman, and A.C. Gosard, Science **283**, 1905 (1999).
 - ⁶ L. DiCarlo, C.M. Marcus, J.S. Harris, Jr., Phys. Rev. Lett. **91**, 246804 (2003).
 - ⁷ S.K. Watson, R.M. Potok, C.M. Marcus, and V. Umansky, Phys. Rev. Lett. **91**, 258301 (2003).
 - ⁸ P.J. Leek, M.R. Buitelaar, V.I. Talyanskii, C.G. Smith, D. Anderson, G.A.C. Jones, J. Wei, and D.H. Cobden, Phys. Rev. Lett. **95**, 256802 (2005).
 - ⁹ W.G. van der Wiel, S.De Franceschi, J.M. Elzerman, T. Fujisawa, S. Tarucha, and L.P. Kouwenhoven, Rev. Mod. Phys. **75**, 1 (2003).
 - ¹⁰ L.P. Kouwenhoven, A.T. Johnson, N.C. van der Vaart, C.J.P.M. Harmans, and C.T. Foxon, Phys. Rev. Lett. **67**, 1626 (1991).
 - ¹¹ M.D. Blumenthal, B. Kaestner, L. Li, S. Giblin, T.J.B. M. Janssen, M. Pepper, D. Anderson, G. Jones, and D.A. Ritchie, Nature Phys. **3**, 343 (2007); B. Kaestner, V. Kashcheyevs, S. Amakawa, M.D. Blumenthal, L. Li, T.J.B.M. Janssen, G. Hein, K. Pierz, T. Weimann, U. Siegner, and H.W. Schumacher, Phys. Rev. B **77**, 153301 (2008).
 - ¹² L. Nevou, V. Liverini, P. Friedli, F. Castellano, A. Bismuto, H. Sigg, F. Gramm, E. Müller, and J. Faist, Nature Phys. **7**, 423 (2011).
 - ¹³ F. Hohls, A. C. Welker, Ch. Leicht, L. Fricke, B. Kaestner, P. Mirovsky, A. Müller, K. Pierz, U. Siegner, and H.W. Schumacher, Phys. Rev. Lett. **109**, 056802 (2012).
 - ¹⁴ S. Kohler, J. Lehmann, and P. Hängi, Phys. Rep. **406**, 379 (2005).
 - ¹⁵ P.W. Brouwer, Phys. Rev. B **58**, R10135 (1998).
 - ¹⁶ M. Moskalets and M. Büttiker, Phys. Rev. B **66**, 205320 (2002); **69**, 205316 (2004).
 - ¹⁷ A.-P. Jauho, N.S. Wingreen, and Y. Meir, Phys. Rev. B **50**, 5528 (1994).
 - ¹⁸ G. Stefanucci and C.-O. Almbladh, Phys. Rev. B **69**, 195318 (2004); S. Kurth, G. Stefanucci, C.-O. Almbladh, A. Rubio, and E.K.U. Gross, Phys. Rev. B **72**, 035308 (2005); G. Stefanucci, S. Kurth, A. Rubio, and E.K.U. Gross, Phys. Rev. B **77**, 075339 (2008).
 - ¹⁹ Y. Zhu, J. Maciejko, T. Ji, H. Guo, and J. Wang, Phys. Rev. B **71**, 075317 (2005).
 - ²⁰ J. Maciejko, J. Wang, and H. Guo, Phys. Rev. B **74**, 085324 (2006).
 - ²¹ X. Zheng, F. Wang, C.Y. Yam, Y. Mo, and G.H. Chen, Phys. Rev. B **75**, 195127 (2007).
 - ²² V. Moldoveanu, V. Gudmundsson, and A. Manolescu, Phys. Rev. B **76**, 085330 (2007); Phys. Rev. B **76**, 165308 (2007).
 - ²³ Y. Xing, B. Wang, J. Wang, Phys. Rev. B **82**, 205112 (2010).
 - ²⁴ A. Schiller and S. Hershfield, Phys. Rev. Lett. **77**, 1821 (1996).

- ²⁵ Y. Goldin and Y. Avishai, Phys. Rev. Lett. **81**, 5394 (1998); Phys. Rev. B **61**, 16750 (2000).
- ²⁶ A. Kaminski, Yu.V. Nazarov, and L.I. Glazman, Phys. Rev. Lett. **83**, 384 (1999).
- ²⁷ R. López, R. Aguado, G. Platero, and C. Tejedor, Phys. Rev. Lett. **81**, 4688 (1998).
- ²⁸ R. López, R. Aguado, G. Platero, and C. Tejedor, Phys. Rev. B **64**, 075319 (2001).
- ²⁹ P. Nordlander, M. Pustilnik, Y. Meir, N.S. Wingreen, and D.C. Langreth, Phys. Rev. Lett. **83**, 808 (1999); P. Nordlander, N.S. Wingreen, Y. Meir, and D.C. Langreth, Phys. Rev. B **61**, 2146 (2000).
- ³⁰ M. Plihal, D.C. Langreth, and P. Nordlander, Phys. Rev. B **61**, R13341 (2000).
- ³¹ A. Schiller and S. Hershfield, Phys. Rev. B **62**, R16271 (2000).
- ³² T.L. Schmidt, P. Werner, L. Mühlbacher, and A. Komnik, Phys. Rev. B **78**, 235110 (2008).
- ³³ R. Egger, L. Mühlbacher, and C.H. Mak, Phys. Rev. E **61**, 5961 (2000); H. Wang and M. Thoss, J. Chem. Phys. **119**, 1289 (2003); L. Mühlbacher and E. Rabani, Phys. Rev. Lett. **100**, 176403 (2008); G. Cohen, E. Gull, D.R. Reichman, A.J. Millis, and E. Rabani, Phys. Rev. B **87**, 195108 (2013).
- ³⁴ S. Weiss, J. Eckel, M. Thorwart, and R. Egger, Phys. Rev. B **77**, 195316 (2008); R. Hützen, S. Weiss, M. Thorwart, and R. Egger, Phys. Rev. B **85**, 121408 (2012).
- ³⁵ D. Segal, A.J. Millis, and D.R. Reichman, Phys. Rev. B **82**, 205323 (2010).
- ³⁶ K.A. Al-Hassanieh, A.E. Feiguin, J.A. Riera, C.A. Büsser, and E. Dagotto, Phys. Rev. B **73**, 195304 (2006); F. Heidrich-Meisner, A.E. Feiguin, and E. Dagotto, Phys. Rev. B **79**, 235336 (2009); C.A. Büsser and F. Heidrich-Meisner, Phys. Rev. Lett. **111**, 246807 (2013).
- ³⁷ E. Boulat, H. Saleur, and P. Schmitteckert, Phys. Rev. Lett. **101**, 140601 (2008).
- ³⁸ F. Güttge, F.B. Anders, U. Schollwöck, E. Eidelstein, and A. Schiller, Phys. Rev. B **87**, 115115 (2013).
- ³⁹ H. Schoeller and G. Schön, Phys. Rev. B **50**, 18436 (1994); J. König, J. Schmid, H. Schoeller, and G. Schön, Phys. Rev. B **54**, 16820 (1996); J. König, H. Schoeller, and G. Schön, Phys. Rev. Lett. **76**, 1715 (1996); Phys. Rev. Lett. **78**, 4482 (1997); H. Schoeller, *Mesoscopic Electron transport* (Kluwer, Dordrecht, 1997), p. 291.
- ⁴⁰ J. Splettstoesser, M. Governale, J. König, and R. Fazio, Phys. Rev. B **74**, 085305 (2006); F. Reckermann, J. Splettstoesser, and M.R. Wegewijs, Phys. Rev. Lett. **104**, 226803 (2010).
- ⁴¹ F. Cavaliere, M. Governale, and J. König, Phys. Rev. Lett. **103**, 136801 (2009).
- ⁴² S.A. Gurvitz and Ya.S. Prager, Phys. Rev. B **53**, 15932 (1996).
- ⁴³ B. Dong, H.L. Cui, and X.L. Lei, Phys. Rev. B **69**, 035324 (2004); B. Dong, X.L. Lei, and N.J.M. Horing, Phys. Rev. B **77**, 085309 (2008).
- ⁴⁴ B. Dong, I. Djuric, H.L. Cui, and X.L. Lei, J. Phys.: Condens. Matter **16**, 4303 (2004).
- ⁴⁵ B. Dong, N.J.M. Horing, and H.L. Cui, Phys. Rev. B **72**, 165326 (2005).
- ⁴⁶ J.N. Pedersen and A. Wacker, Phys. Rev. B **72**, 195330 (2005); J.N. Pedersen, B. Lassen, A. Wacker, and M.H. Hettler, Phys. Rev. B **75**, 235314 (2007); J.N. Pedersen and A. Wacker, Physica E **42**, 595 (2010); O. Karlström, C. Emary, P. Zedler, J.M. Pedersen, C. Bergenfeldt, P. Samuelsson, T. Brandes, and A. Wacker, J. Phys. A: Math. Theor. **46**, 065301 (2013).
- ⁴⁷ U. Harbola, M. Esposito, and S. Mukamel, Phys. Rev. B **74**, 235309 (2006).
- ⁴⁸ S. Welack, M. Schreiber, and U. Kleinekathöfer, J. Chem. Phys. **124**, 044712 (2006).
- ⁴⁹ C. Timm, Phys. Rev. B **77**, 195416 (2008).
- ⁵⁰ J.S. Jin, X. Zheng, and Y.J. Yan, J. Chem. Phys. **128**, 234703 (2008).
- ⁵¹ Z.H. Li, N.H. Tong, X. Zheng, D. Hou, J.H. Wei, J. Hu, and Y.J. Yan, Phys. Rev. Lett. **109**, 266403 (2012); S. Wang, X. Zheng, J. Jin, and Y.J. Yan, Phys. Rev. B **88**, 035129 (2013).
- ⁵² V. Moldoveanu, A. Manolescu, and V. Gudmundsson, New J. Phys. **11**, 073019 (2009); V. Gudmundsson, C. Gainar, C.-S. Tang, V. Moldoveanu, and A. Manolescu, New J. Phys. **11**, 113007 (2009); V. Moldoveanu, A. Manolescu, C.S. Tang, and V. Gudmundsson, Phys. Rev. B **81**, 155442 (2010).
- ⁵³ S. Koller, M. Grifoni, M. Leijnse, and M.R. Wegewijs, Phys. Rev. B **82**, 235307 (2010); S. Koller, M. Grifoni, and J. Paaske, Phys. Rev. B **85**, 045313 (2012).
- ⁵⁴ A. Croy and U. Saalman, Phys. Rev. B **80**, 245311 (2009).
- ⁵⁵ A. Croy and U. Saalman, Phys. Rev. B **86**, 035330 (2012).
- ⁵⁶ X. Zheng, G.H. Chen, Y. Mo, S.K. Koo, H. Tian, C.Y. Yam, Y.J. Yan, J. Chem. Phys. **133**, 114101 (2010).
- ⁵⁷ H. Xie, F. Jiang, H. Tian, X. Zheng, Y. Kwok, S. Chen, C.Y. Yam, Y.J. Yan, and G.H. Chen, J. Chem. Phys. **137**, 044113 (2012).
- ⁵⁸ B. Popescu, P.B. Woiczikowski, M. Elstner, and U. Kleinekathöfer, Phys. Rev. Lett. **109**, 176802 (2012).
- ⁵⁹ A. Croy, U. Saalman, A.R. Hernández, and C.H. Lewenkopf, Phys. Rev. B **85**, 035309 (2012).
- ⁶⁰ C. Lacroix, J. Phys. F: Met. Phys. **11**, 2389 (1981); J. Appl. Phys. **53**, 2131 (1982).
- ⁶¹ Y. Meir, N.S. Wingreen, and P.A. Lee, Phys. Rev. Lett. **66**, 3048 (1991).
- ⁶² O. Entin-Wohlman, A. Aharony, and Y. Meir, Phys. Rev. B **71**, 035333 (2005).
- ⁶³ V. Kashcheyevs, A. Aharony, and O. Entin-Wohlman, Phys. Rev. B **73**, 125338 (2006).
- ⁶⁴ R. VanRoermund, S.Y. Shiau, and M. Lavagna, Phys. Rev. B **81**, 165115 (2010).
- ⁶⁵ Z. Zou and P.W. Anderson, Phys. Rev. B **37**, 627 (1988).
- ⁶⁶ J.C. LeGuillou and E. Ragoucy, Phys. Rev. B **52**, 2403 (1995).
- ⁶⁷ T. Ozaki, Phys. Rev. B **75**, 035123 (2007).
- ⁶⁸ A. Croy and U. Saalman, Phys. Rev. B **80**, 073102 (2009).
- ⁶⁹ C. Karrasch, V. Meden, and K. Schönhammer, Phys. Rev. B **82**, 125114 (2010).
- ⁷⁰ J. Hu, R.X. Xu, and Y.J. Yan, J. Chem. Phys. **133**, 101106 (2010).
- ⁷¹ Y. Fu and S.C. Dudley, Phys. Rev. Lett. **70**, 65 (1993).